Published in final edited form as:

Curr Biol. 2022 April 11; 32(7): 1534–1547.e9. doi:10.1016/j.cub.2022.02.022.

Identification of 14-3-3 Proteins, Polo kinase, and RNA-binding protein Pes4 as Key Regulators of Meiotic Commitment in Budding Yeast

Janardan N. Gavade[1], **Chris M. Puccia**[1], **S. Grace Herod**[2], **Jonathan C. Trinidad**[3], **Luke E. Berchowitz**[2], **Soni Lacefield**[1,4,*]

[1]Indiana University, Department of Biology, Bloomington, IN USA

[2]Columbia University Irving Medical Center, Department of Genetics and Development, Hammer Health Sciences Center, New York, NY USA

[3]Indiana University, Department of Chemistry, Bloomington, IN USA

[4]Lead Contact

Summary

The initiation of the cell division process of meiosis requires exogenous signals that activate internal gene regulatory networks. Meiotic commitment ensures the irreversible continuation of meiosis, even upon withdrawal of the meiosis-inducing signals. A loss of meiotic commitment can cause highly abnormal polyploid cells and can ultimately lead to germ cell tumors. Despite the importance of meiotic commitment, only a few genes involved in commitment are known. In this study, we have discovered six new regulators of meiotic commitment in budding yeast, including Bcy1, which is involved in nutrient sensing, the meiosis-specific kinase Ime2, Polo kinase Cdc5, RNA-binding protein Pes4, and the 14-3-3 proteins Bmh1 and Bmh2. Decreased levels of these proteins cause a failure to establish or maintain meiotic commitment. Importantly, we found that Bmh1 and Bmh2 are involved in multiple processes throughout meiosis and in meiotic commitment. First, cells depleted of both Bmh1 and Bmh2 trigger the pachytene checkpoint, likely due to a role in DNA double strand break repair. Second, Bmh1 interacts directly with the middle meiosis transcription factor Ndt80 and both Bmh1 and Bmh2 maintain Ndt80 levels. Third, Bmh1 and Bmh2 bind Cdc5 and enhance its kinase activity. Finally, Bmh1 binds Pes4, which regulates the timing of the translation of several mRNAs in meiosis II and is required to maintain meiotic commitment. Our results demonstrate that meiotic commitment is actively maintained

*Correspondance: Soni Lacefield, sonil@indiana.edu, Indiana University, 1001 E. 3rd Street, Bloomington, IN 47405, @LacefieldLab, Phone:812-856-2429.

Author Contributions

SL and JG wrote the manuscript. GH and LB contributed the Cdc5 kinase assay. JT contributed the mass spectrometry analysis. JG, CP, and SL collected and analyzed all other data.

Declaration of Interests

The authors do not have any competing interests to declare.

throughout meiosis with the 14-3-3 proteins and Polo kinase serving as key regulators of this developmental program.

eTOC

Meiotic commitment ensures the continuation of meiosis, even upon withdrawal of the meiosis-inducing signal. Gavade et al. identify six new regulators of meiotic commitment in budding yeast, including 14-3-3 proteins, Polo kinase and an RNA-binding protein. Their results demonstrate that commitment is actively maintained throughout meiosis.

Introduction

The production of haploid gametes requires the cell division process of meiosis, in which two rounds of chromosome segregation follow one round of DNA replication. Extrinsic signals induce meiotic entry by activating intrinsic gene regulatory networks[1,2]. Once cells enter meiosis, precise temporal control of meiotic regulators ensure that meiosis events progress in a particular order[3]. For both entry into and maintenance of meiosis, some mitotic cell cycle pathways are inhibited[4–6]. The importance of inhibiting these pathways is shown through the identification of genetic mutants that form germ cell tumors due to the misexpression of mitotic regulators during meiosis. For example, in *C. elegans* and *D. melanogaster*, mutations in the translational repressors GLD-1 and Bruno, respectively, cause inappropriate expression of mitotic cyclins during meiosis. Once expressed, inappropriate activation of cyclin-dependent kinase (CDK) caused cells to enter mitosis, forming germ cell tumors[7,8].

Although these studies have revealed important aspects of meiotic maintenance, we have a limited understanding of the factors ensuring that cells complete meiosis by preventing mitosis. To address this question, we studied meiotic commitment in *S. cerevisiae.* We define meiotic commitment as the point at which the meiosis-inducing signal is no longer required for meiotic completion[9,10]. In budding yeast, starvation is the major meiosis-inducing signal; cells need to remain starved until reaching a commitment point in mid-prometaphase I. Budding yeast is unique in its ability to return to mitosis if the meiosis-inducing signal is not maintained prior to meiotic commitment, in a specialized cell-cycle termed ‘return-to-growth’[2,9,11–14]. If nutrient-rich medium is provided after the commitment, cells complete meiosis, and package meiotic products into spores.

High levels of the Ndt80 transcription factor are important for establishing meiotic commitment in budding yeast[9,10,15]. Ndt80 induces transcription of middle meiosis genes whose protein products are needed for prophase I exit and the meiotic divisions[9,16–19]. Reduced Ndt80 levels results in a commitment defect; upon nutrient-rich medium addition, cells inappropriately exit meiosis after meiosis I, creating multi-nucleate polyploid cells during the subsequent mitotic division[10].

Only a few genes are implicated in meiotic commitment[10,14,20–22]. To identify new meiotic commitment regulators, we performed a genome-scale screen for rescue of meiotic commitment in cells with reduced Ndt80 levels. We identified five proteins needed for

meiotic commitment: Bcy1, a regulator of nutrient sensing; Ime2, a CDK-like kinase; Polo kinase, Cdc5; and 14–3-3 proteins Bmh1 and Bmh2. Importantly, we found that Bmh1 and Bmh2 are involved in multiple processes throughout meiosis that affect the establishment and maintenance of meiotic commitment. Bmh1 and Bmh2 are needed for normal Ndt80 levels, activation of Polo kinase, and interaction with an RNA-binding protein, Pes4, which regulates the timing of translation of several mRNAs important for meiosis II progression. Our study supports a model in which meiotic commitment is actively maintained through multiple processes throughout meiosis.

Results

BCY1, IME2, BMH1, BMH2, and *CDC5* are important for meiotic commitment.

We monitor commitment using a microfluidics setup, which allows us to flow in nutrients at precise meiotic stages. Fluorescent markers show the meiotic stage at the time of nutrient addition in individual cells[10,23,24]. Synaptonemal complex component Zip1-GFP shows the synaptonemal complex assembly and disassembly in prophase I[23,25,26]. GFP-Tub1 marks the spindle and Spc42-mCherry marks the spindle pole bodies (SPBs), allowing the determination of stages beyond prophase I[27]. Although Zip1 and Tub1 are both tagged with GFP, they are easily distinguished due to temporal and morphological differences of the synaptonemal complex and spindle. Cells earlier than mid-prometaphase I are uncommitted and exit meiosis, form a bud, and undergo mitosis upon nutrient addition (Figure 1A-B)[10]. Cells in late prometaphase I and beyond are committed and will finish meiosis upon nutrient addition (Figure 1C-E).

Deleting the mid-sporulation elements within the *NDT80* promoter results in low Ndt80 levels and ablates meiotic commitment[10]. Upon nutrient addition at any meiotic stage, cells underwent mitosis, often causing multi-nucleate polyploid cells (Figure 1F-H)[10]. For ease of discussion, we named this strain “low Ndt80 strain”. The low Ndt80 strain likely fails to commit to meiosis due to low expression of an Ndt80 target. Therefore, we performed a systematic screen to identify genes that rescued meiotic commitment when overexpressed. We expected to identify genes required for establishment of the committed state, genes involved in nutrient sensing, and genes that maintain meiotic commitment by ensuring meiotic progression.

Once the low Ndt80 strain with individual 2μ plasmids from the Yeast Tiling Collection reached meiosis II, we added nutrients, imaged, and scored cells as either uncommitted or committed[28]. Uncommitted cells, such as those with an empty vector, budded and underwent mitosis upon nutrient addition (Figure 1I). Committed cells either remained in or completed meiosis upon nutrient addition (Figure 1C). As a positive control, 2μ-*NDT80* rescued meiotic commitment (Figure 1J-K). Hits were confirmed and individual genes from the plasmids were subcloned and tested for increased commitment in the low Ndt80 strain (Table S1). We focused on five genes: *BCY1, IME2*, *BMH1*, *BMH2*, and *CDC5*. We note that suppression of commitment defects in the low Ndt80 strain does not definitively show that the overexpressed gene is involved in meiotic commitment; many genes whose overexpression promotes progression through meiosis could possibly suppress commitment defects[20]. Therefore, we characterized mutants to reveal a role in meiotic commitment.

Bcy1 and Ime2 ensure meiotic commitment

Identification of *BCY1* and *IME2* in our screen likely corresponds with their known functions in inhibiting the glucose response pathway and activating Ndt80, respectively[29–31]. Bcy1 is a negative regulatory subunit of protein kinase A (PKA), which functions in the RAS/cAMP-dependent signaling pathway induced in response to glucose[31–33]. *BCY1* overexpression in the low Ndt80 strain increased the committed cell population upon nutrient-rich medium addition in metaphase I and beyond (Figure S1A, 1F). Conversely, reducing Bcy1 levels by deleting one copy of *BCY1* in an otherwise wildtype strain resulted in an increased uncommitted cell population when compared to wildtype (Figure S1B, 1E). We could not test the homozygous deletion because meiotic entrance requires some Bcy1[34,35]. Overall, these results demonstrate that meiotic commitment requires full Bcy1 levels, likely by preventing PKA activation.

The meiosis-specific Ime2 kinase activates Ndt80 through phosphorylation[29,30]. Therefore, Ime2's known function is consistent with our finding that *IME2* overexpression increased the population of committed cells when compared to the low Ndt80 strain (Figure S1C,1F). To determine if decreased Ime2 activity causes a loss of commitment in an otherwise wildtype strain, we mutated T242, a residue phosphorylated in Ime2's activation loop for full Ime2 activity[36,37]. Most *ime2-T242A* cells remained in pachytene; those that exited pachytene then arrested at different stages (Figure S1D-E). Because Ime2 also phosphorylates the *NDT80* repressor Sum1 to help relieve repression, we repeated these experiments in *sum1Δ* cells[38–41]. Although most *ime2-T242A sum1Δ* also remained in pachytene, more cells completed meiosis (Figure S1E). Therefore, we performed the commitment assay in *sum1Δ* mutants. Loss of *SUM1* did not affect meiotic commitment (Figure S1F). In contrast, *ime2-T242A sum1Δ* mutants had a strong commitment defect (Figure S1G). Overall, our results demonstrate that full Ime2 activity is required for meiotic commitment.

Bmh1 and Bmh2 Are Required for Full Ndt80 Expression and Commitment

We next focused on *BMH1* and *BMH2*, which encode the budding yeast 14-3-3 proteins[42–44]. 14-3-3 proteins typically bind phosphorylated residues on proteins to modulate their activity, stimulate protein-protein interactions, regulate sub-cellular localization, affect their stability, and facilitate chaperone-like activities[45–51]. *BMH1* or *BMH2* overexpression resulted in more committed cells in the low Ndt80 strain (Figure 2A-C, 1F). These cells were committed, but they either stayed arrested in meiosis I or meiosis II after nutrient addition (Figure 2C). Wildtype cells overexpressing *BMH1* were committed and finished meiosis, showing that Bmh1 overexpression does not cause an arrest (Figure S2A). Therefore, the committed low Ndt80 cells overexpressing Bmh1 may not have enough Ndt80 to complete meiosis upon nutrient addition.

We analyzed deletion mutants to determine if *BMH1* and *BMH2* are required for meiotic commitment. Previous reports showed that *bmh1Δ* and *bmh2Δ* mutants exhibit minor sporulation and spore viability defects, but did not implicate a possible role for the proteins in meiotic commitment[52,53]. Both *bmh1Δ* and *bmh2Δ* strains underwent meiosis with normal timing (Figure S2B-C). However, they were defective for meiotic commitment upon

nutrient addition in metaphase I and anaphase I (Figure 2D-G). We observed two phenotypes of uncommitted cells upon nutrient addition in prometaphase I or metaphase I: i) cells formed a bud and underwent mitosis (Figure 2D); or, ii) cells underwent meiosis I, formed a bud and then underwent mitosis with two spindles (Figure 2E).

Phosphorylation of a conserved residue within the C-terminus of 14-3-3 proteins is important for efficient binding[54–57]. In Bmh1, S235 resides in a patch of highly conserved amino acids among 14-3-3 orthologs (Figure S2D). To determine if Bmh1 phosphorylation is important for meiotic commitment, we mutated S235, and due to proximity, S238 and S240 (*bmh1–3A*). *bmh1–3A* cells had an increased population of uncommitted cells when compared to wildtype upon nutrient addition in metaphase I and anaphase I (Figure S2E, 1E). Therefore, Bmh1's conserved serine residues are required for meiotic commitment.

Because *BMH1* and *BMH2* are paralogs with redundant functions, we hypothesized that some cells remained committed in the single mutants due to the presence of the other paralog[44]. The double knockout is inviable in our strain background. Therefore, we made a meiotic depletion allele by placing *BMH1* under control of the mitosis-specific *CLB2* promoter in a *bmh2Δ* strain (*bmh1-md bmh2Δ*). 80% of *bmh1-md bmh2Δ* cells arrested at pachytene, scored by Zip1-GFP presence (Figure 2H-I). Because the *bmh1-md bmh2Δ* cells enter prophase I, unlike double knockouts reported in a different strain background[52], we assume that a minor amount of Bmh1 is present. The 20% of *bmh1-md bmh2Δ* cells that exited prophase I then arrested at different meiotic stages, demonstrating that Bmh1 and Bmh2 have important functions throughout meiosis (Figure S2F).

We asked whether the pachytene arrested *bmh1-md bmh2Δ* cells triggered the pachytene checkpoint. We deleted two genes important for checkpoint signaling, *MEK1* and *MEC1*. Mek1is a meiosis-specific checkpoint kinase downstream of the signal[58–61]. Mec1 responds to DNA damage and transduces the checkpoint signal[62–64]. *MEC1* is essential, but *mec1Δ* cells can survive with *SML1* deletion[65]. The majority of *bmh1-md bmh2Δ mek1Δ* and *bmh1-md bmh2Δ mec1Δ sml1Δ* cells exit prophase I, demonstrating that arrested cells activated the pachytene checkpoint (Figure 2H). To determine if the pachytene checkpoint arrest was due to unrepaired programmed double strand breaks (DSBs), we deleted *SPO11*, which encodes the enzyme that makes meiotic programmed DSBs[66]. The majority of *bmh1-md bmh2Δ spo11Δ* cells exit prophase I, suggesting that Bmh1 and Bmh2 have important roles in DSB repair (Figure 2H). Although this function is intriguing, we are focusing on Bmh1 and Bmh2's roles in meiotic commitment.

We considered that Bmh1 and Bmh2 could directly interact with Ndt80. Using a two-hybrid assay, we identified an interaction between *BMH1* and a *NDT80* fragment (amino acids 287–627) lacking the DNA-binding domain (Figure 3A)[59,67]. Therefore, Bmh1 could regulate Ndt80 through binding.

Because Ndt80 increases its own transcription, decreased Ndt80 activity or localization would cause decreased Ndt80 protein levels[9,10,16,68]. Therefore, we measured Ndt80 levels in *bmh1Δ* and *bmh2Δ* strains. We arrested cells at metaphase I to ensure that cells are at the same meiotic stage; we made a meiotic null allele of *CDC20*, a co-activator of the APC/C, in

which the mitosis-specific *CLB2* promoter replaced the *CDC20* promoter (*cdc20-mn*)[69–72]. Ndt80 levels were strongly reduced in *bmh1Δ cdc20-mn* and *bmh2Δ cdc20-mn* cells when compared to *cdc20-mn* cells (Figure 3B-C, quantification in Figure S3A-B). Furthermore, Clb1 and Cdc5 levels, whose production is dependent on Ndt80, were reduced in *bmh1Δ cdc20-mn* and *bmh2Δ cdc20-mn* compared to *cdc20-mn* cells (Figure 3B-C, quantification in Figure S3C-F).

Because 14-3-3 proteins can affect the proteins they bind, we asked if the low Ndt80 strain overexpressing Bmh1 or Bmh2 had increased levels of Ndt80 and Ndt80 target proteins[48]. We found that the low Ndt80 strains with 2μ-*BMH1* or 2μ-*BMH2* had increased levels of Ndt80 and the Ndt80 targets Clb1 and Cdc5 when compared to the low Ndt80 strain (Figure 3D-G; $p<0.05$). These results suggest that *BMH1* and *BMH2* overexpression suppressed the commitment defect of the low Ndt80 strain by increasing levels of Ndt80 and Ndt80-dependent targets. Furthermore, addition of 2μ-*NDT80* rescued meiotic commitment in *bmh1Δ* and *bmh2Δ* cells (Figure 3H-I). Overall, these results support the model that Bmh1 and Bmh2 maintain the Ndt80 levels required for meiotic commitment.

Polo Kinase is Essential for Meiotic Commitment

Overexpression of *CDC5* modestly rescued the low Ndt80 strain (Figure 4A). It is unlikely that Cdc5 regulates meiotic commitment through Ndt80; although Cdc5 phosphorylates Ndt80, loss of Cdc5 activity did not change levels of target gene expression[17,73]. Cdc5 has several important functions in meiosis I, but none that would implicate a role in meiotic commitment[73–75]. Because *CDC5* is essential, we made a meiotic null allele by placing *CDC5* under the control of the mitosis-specific *CLB2* promoter (*cdc5-mn*). Without Cdc5, cells arrest in a metaphase I-like state, with a bipolar spindle[73,74]. Because Cdc5 is important for synaptonemal complex disassembly and sister chromatid kinetochore clamping, the *cdc5-mn* cells arrest with synaptonemal complex and with sister chromatid kinetochores bioriented instead of homologous chromosome kinetochores[73–75] (Figure 4B). We compared *cdc5-mn* cells to *cdc20-mn* cells that also arrest at metaphase I (due to a lack of APC/C activity). Upon nutrient addition, *cdc20-mn* cells were committed and remained arrested at metaphase I, confirming that the arrest does not cause commitment defects (Figure 4C, D). In contrast, 85% of *cdc5-mn* cells exit meiosis, form a bud, and undergo mitosis (Figure 4D, E). These results suggest that Cdc5 is required for meiotic commitment.

Because *cdc5-mn* strains arrest with atypical metaphase I characteristics, we asked if cells that undergo meiosis relatively normally, but with reduced Cdc5 levels, also have a meiotic commitment defect. To this end, we analyzed a *CDC5/cdc5Δ* heterozygote that underwent meiosis normally, albeit somewhat slower (Figure S2B-C). 71% of *CDC5/cdc5Δ* cells were uncommitted upon nutrient addition at metaphase I (Figure 4F). In summary, our results demonstrate that Polo kinase is important for meiotic commitment.

We considered that Cdc5's role in meiotic commitment could occur during the normal meiotic process or could be triggered with nutrient addition. To distinguish between these possibilities, we analyzed strains with an inhibitable allele of *CDC5*, *cdc5-as1*[76,77]. We first compared cells with and without chloromethylketone (CMK) inhibitor addition. Like the *cdc5-mn* strains, CMK addition in prophase I caused a loss of commitment when

nutrients were added at metaphase I (Figure 4G). Without inhibitor, *cdc5-as1* cells remained committed to meiosis. Next, we asked whether Cdc5's main role in meiotic commitment occurred prior to or at the time of nutrient-rich medium addition. We made *cdc5-as1* strains with a *cdc20-mn* to arrest cells in metaphase I. We compared *cdc5-as1 cdc20-mn* cells with inhibitor added at prophase I (early) to cells with inhibitor added at the metaphase I arrest but 30-minutes before nutrient addition (late). With inhibitor added late, cells are committed and remained in metaphase I, unlike the uncommitted cells with early addition of inhibitor (Figure 4H). Because *CDC5* is expressed as cells exit prophase I, we conclude that Cdc5 establishes meiotic commitment in late prometaphase I.

Bmh1/Bmh2 Complexes Activate Cdc5 to Ensure Meiotic Commitment

A previous study identified an interaction between Polo-like kinase 1 (Plk1) and the 14-3-3 isoform zeta that was important for Plk1's role in cytokinesis in human cells[78]. This led us to test an interaction between Cdc5 and Bmh1 using a yeast two-hybrid assay[59,67]. Indeed, we found that Bmh1 and Cdc5 interact (Figure 5A).

Because 14-3-3 proteins regulate numerous signaling pathways, we considered that Bmh1/Bmh2 could modulate Cdc5 activity[79,80]. To test this hypothesis, we performed an *in vitro* kinase assay with immunoprecipitated Cdc5–3V5 with and without purified Bmh1/2 complexes. We monitored Cdc5 autophosphorylation as a measure of kinase activity[81–83]. We observed a low level of Cdc5 autophosphorylation without Bmh proteins (Figure 5B-C). However, with Bmh1/Bmh2 complexes, Cdc5 autophosphorylation increased. Because our negative control (unrelated meiotic protein Rim4-V5) did not show a signal, we can conclude that the observed Cdc5 autophosphorylation is not an artifact of the anti-V5 IP. These results suggest that Bmh1 and Bmh2 enhance Cdc5 activity.

We speculated that if Bmh1 also enhances Cdc5 activity *in vivo*, overexpression of *CDC5* could rescue meiotic commitment in *bmh1Δ* and *bmh2Δ* cells. Our commitment assays showed an increased population of *bmh1Δ* committed cells with *CDC5* overexpression (Figure 5D, 2F). Similarly, *bmh2Δ* cells also had an increased committed cell population with *CDC5* overexpression (Figure 5E, 2G). We conclude that Bmh1 and Bmh2 enhance Cdc5 activity to establish meiotic commitment.

Bmh1 Interacts with RNA-binding protein Pes4 to maintain meiotic commitment

Our results showing an interaction between Bmh1 and Cdc5 led us to consider that Bmh1 may also interact with other proteins involved in meiotic commitment. To identify other proteins, we immunoprecipitated Bmh1 in meiosis and assessed the bound proteins by mass spectrometry. For the immunoprecipitation, we tagged the Bmh1 C-terminus with GFP; the tag did not disrupt Bmh1 function, as assayed by survival and normal growth in a *bmh2Δ* background. We compared the immunoprecipitated proteins from the Bmh1-GFP strain to an untagged control strain. Bmh1 is thought to bind hundreds of phosphorylated proteins in mitotic cells[84]. Therefore, identifying numerous interacting proteins in meiotic cells was not surprising (Table S2). We focused on a relatively low-abundance protein that was previously implicated in meiotic commitment, the RNA-binding protein Pes4. Although Pes4 is not required for meiosis, Pes4 delays translation of a subset of Ndt80-dependent mRNAs until

meiosis II[85]. Importantly, the mRNAs bound by Pes4 are protected from destabilization when cells are exposed to nutrient-rich medium[15,85].

We used co-immunoprecipitation to test the interaction between Pes4 and Bmh1. Immunoprecipitation of Pes4–3HA with anti-HA antibody revealed the presence of Bmh1-GFP, suggesting that they interact (Figure 6A). Because we did not see an interaction between Pes4–3HA and LacI-GFP (unrelated GFP-tagged protein), we can conclude that the observed interaction was not due to an interaction of Pes4 and GFP (Figure 6B).

We next asked if Cdc5 phosphorylates Pes4. We isolated protein from *cdc20-mn* and *cdc5-mn* strains with *PES4–3HA*. We did not detect differences in the mobility of Pes4–3HA by western blot (Figure 6C). However, we identified multiple bands when we added Phostag reagent, which slows the migration of phosphorylated species (Figure 6D). A comparison between the *cdc20-mn* and *cdc5-mn* strains did not show differences in the mobility of the bands, suggesting that Pes4 is likely phosphorylated by other kinases, not Cdc5.

To determine if Pes4 has an important role in meiotic commitment, we performed commitment assays in *pes4Δ* cells. We found an increase in the uncommitted cell population in *pes4Δ* compared to wildtype upon nutrient-rich medium addition (Figure 6E, 1E). Furthermore, *PES4* overexpression in *bmh1Δ* cells decreased the uncommitted cell population when compared to *bmh1Δ* cells (Figure 6F, 2F). In summary, our results support the model that Bmh1 interacts with Pes4 to maintain meiotic commitment.

Discussion

Successful completion of meiosis requires that cells remain committed to meiosis, even in the presence of a mitosis-inducing signal. Historically, meiotic commitment has been studied in budding yeast due to the ease of providing meiotic cells the mitosis-inducing signal: nutrient-rich medium[10–14,20,22,86–88]. However, few genes have been implicated in meiotic commitment[10,14,20–22]. Here, we provide a greater understanding of meiotic commitment by identifying six new factors required for meiotic commitment: Bcy1, Ime2, Bmh1, Bmh2, Cdc5, and Pes4. These proteins either establish meiotic commitment (Ime2, Bmh1, Bmh2, Cdc5), maintain meiotic processes for commitment (Bmh1, Bmh2, Pes4), or block the mitosis-inducing signal (Bcy1). Strikingly, our results suggest that commitment does not occur at one point but instead is actively maintained throughout meiosis.

Bcy1, is the negative regulatory subunit of PKA, a kinase involved in RAS/cAMP-dependent signaling that leads to increased gene expression in response to glucose[33,89]. A previous study found an upregulation of *BCY1* expression upon nutrient addition to committed cells[15]. Furthermore, gene expression patterns that were altered in response to PKA activity in vegetative cells were not altered in committed cells, suggesting that committed cells do not activate PKA. Overexpression of *BCY1* increased committed cell populations in the low Ndt80 strain (Figure S1A). Conversely, loss of one copy of *BCY1* in an otherwise wildtype strain resulted in uncommitted cells (Figure S1B). Therefore, these combined data suggest that increased Bcy1 levels in committed cells ensures meiotic commitment by blocking the response to nutrients.

The other genes identified in the screen, *IME2, BMH1, BMH2,* and *CDC5* establish meiotic commitment through their roles in meiosis. Only Ime2 had an obvious connection to meiotic commitment. Ime2 phosphorylates and activates Ndt80 to further induce transcription of the middle meiosis genes[29,30,36]. An Ime2 mutant with decreased activity had a strong commitment defect (Figure S1G). Therefore, Ime2 is important for meiotic commitment likely through activating Ndt80, which increases Ndt80 and Ndt80-dependent transcript levels.

We identified Bmh1 and Bmh2 as key regulators of meiotic commitment, through multiple mechanisms. First, Bmh1 and Ndt80 interact and *bmh1Δ* and *bmh2Δ* strains have decreased Ndt80 levels (Figure 3A-C). Overexpression of *BMH1* and *BMH2* increased Ndt80 levels in the low Ndt80 strain, which lacks Ndt80 binding sites within the promoter (Figure 3D-E). Therefore, the increased levels are not likely due to increased transcription. Our data is consistent with a model that Bmh1 and Bmh2 stabilize Ndt80.

Second, Bmh1 interacts with Cdc5 and enhances Cdc5 autophosphorylation, which further activates Cdc5 (Figure 5A-C). Loss of Cdc5 activity, either with a meiotic null allele or an inhibitable allele, causes a failure of meiotic commitment (Figure 4D-G). Cdc5 activity during prometaphase/metaphase I protect meiotic commitment (Figure 4H). These results suggest that a normal meiotic role of Cdc5 may be required for meiotic commitment. An interesting future direction is to identify Cdc5 substrates needed for meiotic commitment.

Finally, we identified an interaction between Bmh1 and RNA-binding protein Pes4. Pes4 delays translation of approximately 30 Ndt80-dependent transcripts until meiosis II[85]. Additionally, upon nutrient addition, Pes4 protects the bound mRNA transcripts[15,85]. We found that a large population of *pes4Δ* cells failed to maintain meiotic commitment (Figure 6E). Furthermore, *PES4* overexpression increased the population of committed *bmh1Δ* cells (Figure 6F). Combined, these results suggest that Pes4 maintains meiotic commitment by protecting transcripts whose encoded proteins are needed in meiosis II.

Our results support a model in which Bmh1, Bmh2, and Cdc5 are central regulators of meiotic commitment by preventing cells from escaping meiosis upon nutrient addition (Figure 6G). As cells exit prophase I, Ime2 activates Ndt80, which leads to the transcription of *CDC5*, *PES4,* and more *IME2*. Bmh1 and Bmh2 interact with Ndt80, Cdc5, and Pes4 for meiotic commitment. First, Bmh1 and Bmh2 are needed for normal Ndt80 levels. Second, Bmh1/2 complexes enhance Cdc5 kinase activity. Third, Bmh1 and Pes4 interact, possibly enhancing Pes4's ability to protect mRNAs and ensure their delayed translation in meiosis II. Intriguingly, Pes4 only becomes essential for meiotic progression in the presence of nutrient-rich medium. Therefore, this work raises the exciting possibility that the temporal regulation of translation by an RNA-binding protein has evolved to ensure that cells complete meiosis when exposed to a mitosis-inducing signal.

STAR Methods

RESOURCE AVAILABILITY

Lead Contact—Further information and requests for resources and reagents should be directed to and will be fulfilled by the lead contact, Soni Lacefield (sonil@indiana.edu).

Materials Availability—All budding yeast strains and plasmids used in this study will be made available upon request without any restriction.

Data Availability

- The data reported in this paper will be shared by the lead contact upon request.
- This paper does not report original code.
- Any additional information required to reanalyze the data reported in this paper is available from the lead contact upon request.

EXPERIMENTAL MODEL AND SUBJECT DETAILS

Budding yeast strains—Unless noted, *Saccharomyces cerevisiae* strains used in this study are derivatives of W303 (*ade2–1 can1–100 leu2–3, 112 his3–11, 15 ura3–1 trp1–1*) and can be found in the Key Resource Table. The strains used for the yeast two-hybrid experiment were derivatives of L40 (*his3Δ200 trp1–90 leu2–3,112 ade2 lys2::lexA$_{op}$-HIS3::LYS2 gal80 ura3:: lexA$_{op}$-lacZ::URA3*) with the *GAD* and *lexA* plasmids transformed in. Standard PCR-based methods were used for deleting and tagging genes and swapping promoters[90,91]. The low Ndt80 strain, with the deletion of the MSEs in the promoter, was from a previous study[10]. The *mec1Δ sml1Δ* mutations were introduced in the strain LY6981 by crossing in and mating subsequent haploids. The *CDC5/cdc5* heterozygous strain was created by deleting *CDC5* in a diploid strain. The haploid *cdc5-as1* strain carrying *cdc5L158G* was a gift from the Marston lab and crossed into strains. The *bmh1–3A* strain was constructed by integrating pLB519 in the haploid *bmh1Δ* strains at the *BMH1* promoter.

Media—The following yeast media were used in this study: YPD (2% peptone, 1% yeast extract, 2% glucose), YPA (2% peptone, 1% yeast extract, 2% potassium acetate), SPM (1% potassium acetate), SCD –leu (0.67% YNB without amino acids, 0.2% dropout mix containing all amino acids except leucine, 2% glucose), SCA –leu (0.67% YNB without amino acids, 0.2% dropout mix containing all amino acids except leucine, 2% potassium acetate), SCD –ura (0.67% YNB without amino acids, 0.2% dropout mix containing all amino acids except uracil, 2% glucose), SCA –ura (0.67% YNB without amino acids, 0.2% dropout mix containing all amino acids except uracil, 2% potassium acetate), SCD-leu-trp (0.67% YNB without amino acids, 0.2% dropout mix containing all amino acids except leucine and tryptophan, 2% glucose), and 2XSC (1.34% YNB without amino acids, 0.4% dropout mix containing all amino acids, 4% glucose).

METHOD DETAILS

Plasmid construction—Oligos and plasmids can be found in Tables S3 and Key Resource Table, respectively. Empty 2μ vector (pLB227) was made from the A4 plasmid from the Yeast Genomic Tiling Collection by digesting with SpeI and NheI and religating the 6.5kb fragment[28]. *P_{NDT80}-NDT80:LEU2* (pLB225) was made by digesting the A6 plasmid from the Yeast Genomic Tiling Collection using SalI and SacI and the 7.1 kb band was ligated into cut pLB107. *P_{BMH1}-BMH1:LEU2* (pLB262) was made by amplifying *P_{BMH1}-BMH1* using oligos LO1677 and LO1678. The fragment was digested with SalI and BamHI and ligated with cut YEplac181. *P_{BMH2}-BMH2:LEU2* (pLB539) was made by amplifying *P_{BMH2}-BMH2* using oligos LO1968 and LO1969, digesting with SalI and XmaI and ligating into cut YEplac181. *lexA-BMH1:TRP1* (pLB518) was made by amplifying *BMH1* ORF using oligos LO3089 and LO3090, digesting with EcoRI and SalI and ligating into cut pBTM116. *GAL4AD-CDC5:LEU2* (pLB491) was made by amplifying the *CDC5* ORF using LO3062 and LO3063 and ligating with NcoI and XhoI digested pACTII. *P_{CDC5}-CDC5:URA3* (pLB465) and *P_{CDC5}-CDC5:LEU2* (pLB463) were made by amplifying the *P_{CDC5}-CDC5* ORF with oligos LO2800 and LO2801, and ligating into BamHI and SacI digested YEPlac195 and YEplac181 respectively. *P_{BMH1}-BMH1* was amplified with LO1677 and LO1678, and cloned in SalI and BamHI digested pRS403 (ref Sikorski and Heiter, 1989). *P_{BMH1}-bmh1–3A:HIS3* (pLB519) was made by Genewiz, using *P_{BMH1}-BMH1:HIS3* (pLB509) as a template. *P_{PES4}-PES4:URA3* (pLB513) was made by amplifying *P_{PES4}-PES4* with oligos LO3163 and LO3164 and ligating in SalI and SacI digested YEplac195. *P_{BCY1}-BCY1:LEU2* (pLB306) was made by amplifying *P_{BCY1}-BCY1* with oligos LO1808 and LO1809 and ligating in SalI and BamHI digested YEplac181. *P_{IME2}-IME2:LEU2* (pLB258) was made by amplifying *P_{IME2}-IME2* with oligos LO1673 and LO1674 and ligating into SalI and XmaI digested YEplac181. *P_{IME2}-IME2-myc-TRP1* (pLB268) was made by amplifying *P_{IME2}-IME2-myc* using oligos LO686 and LO687. *P_{IME2}-IME2 T242A-myc-TRP1* (pLB285) was made by using pLB268 as a template and oligos LO1627 and LO1629 for site-directed mutagenesis.

Commitment assay—Cells were grown in YPD for 16–18 hours at 30°C, transferred to YPA (1:50 dilution) for 12–14 hours at 30°C, washed once with sterile water, resuspended in SPM and incubated on a roller drum at 25°C for 9:30 hours (except the low Ndt80 strain background was incubated for 13:30 hours and *cdc20mn*, *cdc5mn* and *cdc5-as1* strains were incubated for 12–14 hours). Cells were then loaded into the microfluidics chambers (CellAsic Y04D yeast perfusion plates). For inhibition of Cdc5 in the *cdc5-as1* strain, 5μM chloromethylketone (CMK) inhibitor (gift of A. Marston) was added in the culture tube 10 minutes prior to loading and was also added to 2XSC. SPM flowed through the chamber for 20 minutes and cells were exposed to 2XSC 10hrs after SPM addition, (14hrs for the low Ndt80 strain background and 12–14 hrs for the *cdc20mn*, *cdc5mn* and *cdc5-as1* strains). The commitment assay was performed using the CellAsic Onix microfluidics perfusion platform.

Meiosis timings—Cells were grown in YPD for 16–18 hours at 30°C, transferred to YPA (1:50 dilution) for 12–14 hours at 30°C, washed once with sterile water, resuspended in SPM and incubated on a roller drum at 25°C for 8 hours. After 8 hours, cells were loaded in a chamber mounted on a coverslip coated with 5μL of concanavalin A (Sigma).

A monolayer of cells was prepared by using 5% agar pad containing potassium acetate. The agar pad was removed before imaging by floating the pad in preconditioned potassium acetate media.

Microscope image acquisition—Cells were imaged using a Nikon Ti-E inverted microscope equipped with SNAPHQ2 CCD camera (Photometrics), 60X oil objective (PlanAPO VC, 1.4NA). For each experiment, 30 random fields were selected. Five z-steps (1.2μm) were acquired for each field. Images were acquired in 10 minutes interval for 8–12 hours. The exposure times for Brightfield was 60ms, 500–700ms for GFP and 700–900ms for mCherry. Z-stacks were combined into a single maximum intensity projection with NIS-Elements software (Nikon).

Overexpression screen—The overexpression screen was performed in 96-well dishes. The low Ndt80 strain was transformed with the Yeast Genomic Tiling Collection[28] in 96-well dishes using the following protocol[92]: Cells were grown in 20mL of YPD for 12 hours at 30°C. 2.5×10^8 cells were transferred to 50ml of pre-warmed YPD and incubated at 30°C for 4 hours. 200uL of the cell suspension was transferred to 96-well plates and the plates were centrifuged for 10 minutes at 1300g. The supernatant was discarded. 5μL of the plasmids from the Yeast Genomic Tiling Collection was placed in each well. 35μL of the transformation mix (15μL of 1M Lithium acetate + 20μL of boiled 2mg/mL salmon sperm DNA) and 100μL of 50% PEG (MW 3350) was added to the cell pellet and incubated at 42°C for 2 hours. The plate was centrifuged at 1300g for 10 minutes, 10μL of sterile water was added to the cells and 5μL of cells were spotted on SC-leu plates. The plates were incubated at 30°C for 2–4 days.

For commitment assays in 96-well dishes, 1mL of SCD-leu was added to each well in a sterile 96-well block. A single colony was inoculated and incubated in the 96-well blocks at 30°C for 24 hours. 40uLs was then diluted into 1mL of SCA-leu. The wells contained sterile magnetic stirrers (3mm × 5mm) and the block was incubated at 30°C for 15hrs on a shaker. The block was covered with sterile air permeable covers. The block was spun at 3000RPM for 1 minute. The supernatant was removed, the cells were washed twice with 1mL of sterile water and then resuspended in 1mL of SPM. The block was sealed with an air permeable seal and stirred at 25°C for 20 hours. The block was spun again at 3000RPM for 1 minute and the supernatant was removed and cells were resuspended in 1mL of 2XSC. The block was placed on the magnetic stirrer at 25°C for 8hrs. The block was centrifuged at 3000RPM for 1 minute. The supernatant was discarded and the cells were transferred to a 96-well round bottom plate. The cells were fixed in 150uL of freshly prepared 4% para-formaldehyde.

For imaging in 96-wells, 5μL of the fixed cells were added to each well. To get a monolayer of cells, an agar pad made up of 1.2% agarose in 1XPBS (pH7.4) was placed on the cells. Cells were imaged at room temperature using a Nikon Eclipse Ti inverted microscope equipped with Hamamatsu Orca-Flash4.0 sCMOS camera 60X oil objective (PlanAPO VC, 1.2NA). For each well, 10 random fields were selected. Five z-steps (1.2μm) were acquired for each well. GFP-Tub1 and Spc42-mCherry were imaged with a 500ms exposure and 1 ND filter. Brightfield images were acquired with a 60ms exposure.

Western blotting—For Western blotting analysis of Ndt80, Cdc5, Clb1, Pes4–3HA, and Pgk1, protein extraction was carried out by using a TCA method [93]. 5mLs of meiosis culture was harvested for each timepoint. Cells were spun at 3000RPM for 1 minute. The supernatant was removed and 5mL of ice-cold 10% Trichloroacetic acid (TCA) was added for 10 minutes. Cells were centrifuged at 5000RPM for 1 minute. The supernatant was removed and 1mL of ice-cold acetone was added to the cells. Cells were vortexed and centrifuged at 14000RPM for 1 minute. The supernatant was discarded and this step was repeated twice. Tubes were left open to dry in the hood for 3 hours. For the protein extraction, 200μL of protein breakage buffer (60mM Tris pH 7.5, 1.2mM EDTA pH8, 3.3 mM DTT, Pierce Protease Inhibitor Mini tablet-EDTA free) was added along with 200μL of 0.5mm glass beads. Cells were broken by vortexing six times with 1-minute pulses, with 1-minute on ice in between. 100μL of 3X SDS buffer was added and tubes were boiled for 5 minutes. The supernatant was resolved on SDS PAGE gel at 150V for 90 minutes and transferred onto a PVDF membrane. For determining the phosphorylation status of Pes4–3HA, supernatant was resolved in Phos-tag gel (SDS PAGE gel supplemented with 100 μM Phos-tag™ AAL 107 solution and 20mmol/L $MnCl_2$). The Phos-tag gel was resolved at 5mA for 12 hours. After electrophoresis, the gel is soaked in 1X transfer buffer containing 1mmol/L EDTA for 10 minutes with gentle agitation. Next, the gel is soaked in 1X transfer buffer without EDTA for 10 minutes with gentle agitation and transferred onto a PVDF membrane. The membranes were blocked with 5% milk in 1X TBST.

The primary antibodies used were a rabbit anti-Ndt80 (generous gift of M. Lichten, 1:10000), anti-Pgk1 mouse (Invitrogen, Catalog #459250, 1:10000), anti-Cdc5 goat (Santa Cruz Biotechnology, sc-6733, 1:1000), anti-Clb1 goat (Santa Cruz Biotechnology, sc-7647, 1:1000), anti-HA mouse (Roche, 12CA5, Catalog #11583816001, 1:1000). The secondary antibodies used were ECL-anti-rabbit HRP IgG (GE Healthcare, NA9340V, 1:10000), ECL-anti-mouse HRP IgG (GE Healthcare, NA9310V, 1:10000), anti-goat IgG HRP (R&D Systems, HAF109, 1:5000).

Densitometry analysis of each protein was carried out by using ImageJ software. The individual densitometry values of Ndt80, Cdc5 and Clb1 were divided by the densitometry values of Pgk1 for the Ndt80/Pgk1, Cdc5/Pgk1 and Clb1/Pgk1 ratios. The graphs were generated by using GraphPad Prism software.

Yeast-two hybrid assay—Transformants containing the *GAD* plasmids and *lexA* plasmids were grown in SCD-leu-trp at 30°C for 16–18 hours. LY8522 was grown in SC for 16–18 hours. The cells were diluted 1:10 in sterile water and the optical density at 600nm (OD_{600}) was measured using a spectrophotometer. Culture volumes equivalent to 0.1 OD were set as starting dilution and were further subjected to 10-fold serial dilution. The serial dilutions were then spotted on SC plates, SC –leu-trp plates and SC –leu-trp-his + 10mM 3-aminotriazole (Sigma) plates. The plates were incubated at 30°C for 3–5 days.

14-3-3 C-terminus sequence analysis—The following FASTA sequences were obtained from NCBI protein resource: NP_011104.3, NP_010384.3, NP_594167.1, NP_564249.1, NP_565977.1, NP_001014516.1, NP_001129171.1, NP_724887.2, NP_001240734.1, NP_003395.1, XP_005158144.1, NP_001076267.1 and NP_061223.2.

The sequences were aligned using blastp suite. The sequences around *Saccharomyces cerevisiae* Bmh1 S235, S238 and S240 were aligned with the 14-3-3 protein sequences across different organisms.

Immunoprecipitation and mass spectrometry analysis—Cells were grown for 16–18 hours in 2mL YPD, diluted 1:50 dilutions into 50mL YPA, and incubated at 30°C for 12–14 hours. Cells were washed once with sterile water and resuspended in 50mL SPM and incubated at 25°C. After 10hrs in SPM, cells were spun down and snap frozen in liquid nitrogen. The cell pellet was thawed on ice, 200μL NP40 lysis buffer (50mM Tris pH7.5, 150mM NaCl, 2mM MgCl2, 1%NP-40, 10% glycerol, Pierce Protease Inhibitor Mini tablet-EDTA free) and 200μL of 0.5mm glass beads were added. The cells were lysed by bead beating 6 times for 1min with 1min on ice in between. The tubes were centrifuged at 4°C at 18000 RCF for 10mins. The supernatant was removed and the protein concentration was measured by Bradford assay (Pierce Coomassie Plus Assay kit, Thermo Scientific, Catalog #23236). 25μL of DYNAbeads Protein G (Invitrogen, Catalog # 10003D) was equilibrated for each IP. 1mg of protein, 10μg anti-GFP mouse (Roche, Catalog #11814460001) and 1mL of NP-40 lysis buffer was added to the DYNAbeads tube. IP samples were incubated on a rotor at 4°C for 12 hours. The beads were immobilized by placing the tube against a magnetic bar. The supernatant was removed and the beads were washed with 1mL of NP-40 lysis buffer. The wash steps were repeated twice and 25μL of 3X SDS buffer was added to the beads. The beads were boiled for 5mins. The supernatant was loaded in a 10-well 4–20% Mini-PROTEAN TGX Precast protein gel (BIO-RAD, Catalog #4561094). The gel was run at 150V for 5 minutes. After the mini-run, the gel was washed 3 times for 10 minutes with distilled water. The gel was stained with Imperial Protein Stain (Thermo Fisher, Catalog #24615) for 30 minutes. To remove excess stain, the gel was washed 3 times for 10 minutes in distilled water. The protein band was excised from the gel and analyzed by mass spectrometry.

Gel bands were diced with a razor blade. Samples were washed twice in 50% acetonitrile, 0.1% formic acid and dried down in a SpeedVac concentrator (Thermo Scientific). Disulfide bonds were reduced by incubation for 45 min at 57 °C with a final concentration of 10 mM Tris (2-carboxyethyl) phosphine hydrochloride (Catalog no C4706, Sigma Aldrich). The gels were washed and a final concentration of 20 mM iodoacetamide (Catalog no I6125, Sigma Aldrich) was then added to alkylate these side chains and the reaction was allowed to proceed for one hour in the dark at 21 °C. The gels were washed and dried down. Gel pieces were rehydrated in 25 mM ammonium bicarbonate containing 200 ng of trypsin (V5113, Promega) and the samples were digested for 14 hours at 37 °C. The following day, peptides were extracted twice using 50% acetonitrile in 0.1% formic acid. The extracts were dried down and desalted using zip tips (EMD Millipore).

Samples were analyzed by LC-MS on an Orbitrap Fusion Lumos (ThermoFisher) equipped with an Easy NanoLC1200 HPLC (ThermoFisher). Peptides were separated on a 75 μm × 15 cm Acclaim PepMap100 separating column (Thermo Scientific) downstream of a 2 cm guard column (Thermo Scientific). Buffer A was 0.1% formic acid in water. Buffer B was 0.1% formic acid in 80% acetonitrile. Peptides were separated on a 60 minute gradient from 0% B to 35% B. Peptides were collisionally fragmented using HCD mode. Precursor ions

were measured in the Orbitrap with a resolution of 120,000. Fragment ions were measured in the ion trap. The spray voltage was set at 2.2 kV. Orbitrap MS1 spectra (AGC 1×106) were acquired from 400–1800 m/z followed by data-dependent HCD MS/MS (collision energy 42%, isolation window of 0.7 Da) for a three second cycle time. Charge state screening was enabled to reject unassigned and singly charged ions. A dynamic exclusion time of 60 seconds was used to discriminate against previously selected ions.

The LC-MS/MS data was searched using Proteome Discoverer 2.1. MS spectra were searched against the *Saccharomyces cerevisiae* database downloaded from Uniprot on 4/2018. The database search parameters were set as follows: two missed protease cleavage sites were allowed for trypsin digested with 10 ppm precursor mass tolerance and 0.6 Da for fragment ion quantification tolerance. Oxidation of methionine, pyroglutamine on peptide amino termini and protein N-terminal acetylation were set as variable modifications. Carbamidomethylation (C; +57Da) was set as a static modification. The proteins included in Table S2 had satisfied the following criteria: i) they were only detected in tagged strains or they showed more than or equal to 50-fold difference in the Tag/NoTag ratio when proteins were detected in both tagged and untagged strains; and, ii) they were identified by two or more peptides.

Cdc5 immunoprecipitation/kinase assay—25 ml cultures were pelleted, washed once with Tris (pH 7.5), transferred into a 2 ml tube and snap frozen in liquid nitrogen for later processing. Cells were broken with Zirconia/Silica beads in 200 μL NP40 Lysis Buffer (50 mM Tris pH 7.5, 150 mM NaCl, 1% NP-40, 10% glycerol) containing 1mM DTT and 1× Halt protease and phosphatase inhibitors (Thermo). After breaking, extracts were cleared twice by centrifugation and protein concentration was determined by Bradford assay. Immunoprecipitations were performed in 1 ml diluted extract (800 μg total protein). Cdc5–3V5 and Rim4–3V5 (control non-kinase tagged protein) were immunoprecipitated at 4°C 2 hours using 20 μL of anti-V5-agarose slurry (Sigma). Purifications were washed 4 times with NP40 buffer.

For the kinase reaction, beads were incubated in kinase buffer (25 mM Tris-HCl pH 7.5, 5 mM beta-glycerophosphate, 1 mM dithiothreitol (DTT), 0.1 mM Na_3VO_4, 10 mM $MgCl_2$, 10 mM ATP (non-radioactive) alone or with 8 μM Bmh1/Bmh2 protein complexes purified from yeast. The reaction was initiated by adding 1 ul of [γ–^{32}P] ATP (3000Ci/mmol) to each sample. 5 ul samples were withdrawn after the indicated amount of time. To stop the reaction, 2.5 ul 3 × SDS loading Buffer (9% SDS, 0.75 mM Bromophenol blue, 187.5 mM Tris-HCl pH 6.8, 30% glycerol, and 810 mM β-mercaptoethanol) was added and samples were boiled for 5 mins. Samples were separated on a 10% SDS-PAGE gel and transferred to a nitrocellulose membrane using a semi-dry transfer (Biorad). The membrane was dried, mounted on a phosphor screen, and imaged on a Typhoon imager (GE Healthcare). Immunoprecipitations were analyzed by detection with anti-V5.

Co-immunoprecipitation—For detecting interaction between Pes4–3HA and Bmh1-GFP, the immunoprecipitation protocol described for Bmh1-GFP was used with the following modifications: 1) 4μg anti-HA mouse (12CA5 Roche, Catalog # 11583816001)

used for immunoprecipitating Pes4–3HA. 2) For inputs, 25μL protein sample was mixed with 5μL 3X SDS buffer and boiled for 5 mins. 25μL input sample was loaded in the gel.

For detecting interaction between Pes4–3HA and LacI-GFP, the immunoprecipitation protocol described for Pes4–3HA was used with the following modifications: 50μM copper sulfate was added in SPM at 0 hour for expressing LacI-GFP. After loading the samples in 4–20% Mini-PROTEAN TGX Precast protein gel (BIO-RAD, Catalog #4561094), the samples were resolved at 150V for 90 minutes and transferred onto a PVDF membrane.

The primary antibodies used were rabbit anti-GFP (generous gift of Dr. Claire Walczak, 1:10000), and anti-HA mouse (12CA5 Roche, Catalog # 11583816001, 1:1000). The secondary antibodies used were ECL-anti-rabbit HRP IgG (GE Healthcare, NA9340V, 1:10000), and ECL-anti-mouse HRP IgG (GE Healthcare, NA9310V, 1:10000).

QUANTIFICATION AND STATISTICAL ANALYSIS

All statistical analyses were performed using GraphPad Prism software. For all microscopy data except the meiosis timings data, the individual cell numbers were entered in the contingency tables and two-sided Fisher's exact test was used to determine the significance. The total number of cells analyzed in each graph are indicated in the figure legends. For the meiosis timings data Mann-Whitney test of significance was used. For the protein quantification in Figure 3 and Figure S3, Image J software was used. For the protein quantification in figure 3, statistical significance was determined for t = 14 using an Unpaired t-test with Welch's correction. For the protein quantification in Figure S3, statistical significance was determined using Two-way Anova. Differences among compared data was considered statistically significant if the p-value was <0.05.

Supplementary Material

Refer to Web version on PubMed Central for supplementary material.

Acknowledgements

We thank Nancy Hollingsworth, Michael Lichten, and Adele Marston for strains and reagents, and Rolf Sternglanz for suggestions. We thank the Lacefield lab for insightful comments on the manuscript. We thank the Light Microscopy and Imaging Center at Indiana University, especially Jim Powers for assistance. This research was supported by NIH grant GM105755 to SL and R35GM124633-01 to LEB, and the Hirschl Family Trust grant to LEB.

References

1. van Werven FJ, and Amon A (2011). Regulation of entry into gametogenesis. Philos Trans R Soc Lond B Biol Sci 366, 3521–3531. 10.1098/rstb.2011.0081. [PubMed: 22084379]
2. Kimble J (2011). Molecular regulation of the mitosis/meiosis decision in multicellular organisms. Cold Spring Harb Perspect Biol 3, a002683. 10.1101/cshperspect.a002683. [PubMed: 21646377]
3. MacKenzie AM, and Lacefield S (2020). CDK Regulation of Meiosis: Lessons from S. cerevisiae and S. pombe. Genes (Basel) 11. 10.3390/genes11070723.
4. Weidberg H, Moretto F, Spedale G, Amon A, and van Werven FJ (2016). Nutrient Control of Yeast Gametogenesis Is Mediated by TORC1, PKA and Energy Availability. PLoS Genet 12, e1006075. 10.1371/journal.pgen.1006075. [PubMed: 27272508]

5. Wei Y, Reveal B, Reich J, Laursen WJ, Senger S, Akbar T, Iida-Jones T, Cai W, Jarnik M, and Lilly MA (2014). TORC1 regulators Iml1/GATOR1 and GATOR2 control meiotic entry and oocyte development in Drosophila. Proc Natl Acad Sci U S A 111, E5670–5677. 10.1073/pnas.1419156112. [PubMed: 25512509]
6. Okaz E, Arguello-Miranda O, Bogdanova A, Vinod PK, Lipp JJ, Markova Z, Zagoriy I, Novak B, and Zachariae W (2012). Meiotic prophase requires proteolysis of M phase regulators mediated by the meiosis-specific APC/CAma1. Cell 151, 603–618. 10.1016/j.cell.2012.08.044. [PubMed: 23101628]
7. Sugimura I, and Lilly MA (2006). Bruno inhibits the expression of mitotic cyclins during the prophase I meiotic arrest of Drosophila oocytes. Developmental cell 10, 127–135. 10.1016/j.devcel.2005.10.018. [PubMed: 16399084]
8. Biedermann B, Wright J, Senften M, Kalchhauser I, Sarathy G, Lee MH, and Ciosk R (2009). Translational repression of cyclin E prevents precocious mitosis and embryonic gene activation during C. elegans meiosis. Developmental cell 17, 355–364. 10.1016/j.devcel.2009.08.003. [PubMed: 19758560]
9. Winter E (2012). The Sum1/Ndt80 transcriptional switch and commitment to meiosis in Saccharomyces cerevisiae. Microbiol Mol Biol Rev 76, 1–15. 10.1128/MMBR.05010-11. [PubMed: 22390969]
10. Tsuchiya D, Yang Y, and Lacefield S (2014). Positive feedback of NDT80 expression ensures irreversible meiotic commitment in budding yeast. PLoS Genet 10, e1004398. 10.1371/journal.pgen.1004398. [PubMed: 24901499]
11. Sherman F, and Roman H (1963). Evidence for two types of allelic recombination in yeast. Genetics 48, 255–261. [PubMed: 13977170]
12. Simchen G, Pinon R, and Salts Y (1972). Sporulation in Saccharomyces cerevisiae: premeiotic DNA synthesis, readiness and commitment. Exp Cell Res 75, 207–218. [PubMed: 4564471]
13. Simchen G (2009). Commitment to meiosis: what determines the mode of division in budding yeast? Bioessays 31, 169–177. 10.1002/bies.200800124. [PubMed: 19204989]
14. Esposito RE, and Esposito MS (1974). Genetic recombination and commitment to meiosis in Saccharomyces. Proc Natl Acad Sci U S A 71, 3172–3176. 10.1073/pnas.71.8.3172. [PubMed: 4606582]
15. Friedlander G, Joseph-Strauss D, Carmi M, Zenvirth D, Simchen G, and Barkai N (2006). Modulation of the transcription regulatory program in yeast cells committed to sporulation. Genome Biol 7, R20. 10.1186/gb-2006-7-3-r20. [PubMed: 16542486]
16. Hepworth SR, Friesen H, and Segall J (1998). NDT80 and the meiotic recombination checkpoint regulate expression of middle sporulation-specific genes in Saccharomyces cerevisiae. Molecular and cellular biology 18, 5750–5761. 10.1128/MCB.18.10.5750. [PubMed: 9742092]
17. Chu S, DeRisi J, Eisen M, Mulholland J, Botstein D, Brown PO, and Herskowitz I (1998). The transcriptional program of sporulation in budding yeast. Science 282, 699–705. 10.1126/science.282.5389.699. [PubMed: 9784122]
18. Chu S, and Herskowitz I (1998). Gametogenesis in yeast is regulated by a transcriptional cascade dependent on Ndt80. Mol Cell 1, 685–696. 10.1016/s1097-2765(00)80068-4. [PubMed: 9660952]
19. Xu L, Ajimura M, Padmore R, Klein C, and Kleckner N (1995). NDT80, a meiosis-specific gene required for exit from pachytene in Saccharomyces cerevisiae. Molecular and cellular biology 15, 6572–6581. [PubMed: 8524222]
20. Honigberg SM, and Esposito RE (1994). Reversal of cell determination in yeast meiosis: postcommitment arrest allows return to mitotic growth. Proc Natl Acad Sci U S A 91, 6559–6563. [PubMed: 8022820]
21. Honigberg SM, Conicella C, and Espositio RE (1992). Commitment to meiosis in Saccharomyces cerevisiae: involvement of the SPO14 gene. Genetics 130, 703–716. [PubMed: 1582554]
22. Ballew O, and Lacefield S (2019). The DNA Damage Checkpoint and the Spindle Position Checkpoint Maintain Meiotic Commitment in Saccharomyces cerevisiae. Current biology : CB 29, 449–460 e442. 10.1016/j.cub.2018.12.043. [PubMed: 30686741]

23. Scherthan H, Wang H, Adelfalk C, White EJ, Cowan C, Cande WZ, and Kaback DB (2007). Chromosome mobility during meiotic prophase in Saccharomyces cerevisiae. Proc Natl Acad Sci U S A 104, 16934–16939. 10.1073/pnas.0704860104. [PubMed: 17939997]
24. Carminati JL, and Stearns T (1997). Microtubules orient the mitotic spindle in yeast through dynein-dependent interactions with the cell cortex. J Cell Biol 138, 629–641. 10.1083/jcb.138.3.629. [PubMed: 9245791]
25. Sym M, Engebrecht JA, and Roeder GS (1993). ZIP1 is a synaptonemal complex protein required for meiotic chromosome synapsis. Cell 72, 365–378. 10.1016/0092-8674(93)90114-6. [PubMed: 7916652]
26. White EJ, Cowan C, Cande WZ, and Kaback DB (2004). In vivo analysis of synaptonemal complex formation during yeast meiosis. Genetics 167, 51–63. 10.1534/genetics.167.1.51. [PubMed: 15166136]
27. Tsuchiya D, and Lacefield S (2013). Cdk1 modulation ensures the coordination of cell-cycle events during the switch from meiotic prophase to mitosis. Current biology : CB 23, 1505–1513. 10.1016/j.cub.2013.06.031. [PubMed: 23871241]
28. Jones GM, Stalker J, Humphray S, West A, Cox T, Rogers J, Dunham I, and Prelich G (2008). A systematic library for comprehensive overexpression screens in Saccharomyces cerevisiae. Nat Methods 5, 239–241. 10.1038/nmeth.1181. [PubMed: 18246075]
29. Benjamin KR, Zhang C, Shokat KM, and Herskowitz I (2003). Control of landmark events in meiosis by the CDK Cdc28 and the meiosis-specific kinase Ime2. Genes Dev 17, 1524–1539. 10.1101/gad.1101503. [PubMed: 12783856]
30. Sopko R, Raithatha S, and Stuart D (2002). Phosphorylation and maximal activity of Saccharomyces cerevisiae meiosis-specific transcription factor Ndt80 is dependent on Ime2. Molecular and cellular biology 22, 7024–7040. 10.1128/MCB.22.20.7024-7040.2002. [PubMed: 12242283]
31. Broach JR (2012). Nutritional control of growth and development in yeast. Genetics 192, 73–105. 10.1534/genetics.111.135731. [PubMed: 22964838]
32. Toda T, Cameron S, Sass P, Zoller M, Scott JD, McMullen B, Hurwitz M, Krebs EG, and Wigler M (1987). Cloning and characterization of BCY1, a locus encoding a regulatory subunit of the cyclic AMP-dependent protein kinase in Saccharomyces cerevisiae. Molecular and cellular biology 7, 1371–1377. 10.1128/mcb.7.4.1371-1377.1987. [PubMed: 3037314]
33. Thevelein JM, and de Winde JH (1999). Novel sensing mechanisms and targets for the cAMP-protein kinase A pathway in the yeast Saccharomyces cerevisiae. Mol Microbiol 33, 904–918. 10.1046/j.1365-2958.1999.01538.x. [PubMed: 10476026]
34. Matsuura A, Treinin M, Mitsuzawa H, Kassir Y, Uno I, and Simchen G (1990). The adenylate cyclase/protein kinase cascade regulates entry into meiosis in Saccharomyces cerevisiae through the gene IME1. EMBO J 9, 3225–3232. [PubMed: 2209544]
35. Tripp ML, and Pinon R (1986). Control of the cAMP pathway by the cell cycle start function, CDC25, in Saccharomyces cerevisiae. J Gen Microbiol 132, 1143–1151. 10.1099/00221287-132-5-1143. [PubMed: 3021894]
36. Schindler K, Benjamin KR, Martin A, Boglioli A, Herskowitz I, and Winter E (2003). The Cdk-activating kinase Cak1p promotes meiotic S phase through Ime2p. Molecular and cellular biology 23, 8718–8728. 10.1128/MCB.23.23.8718-8728.2003. [PubMed: 14612412]
37. Schindler K, and Winter E (2006). Phosphorylation of Ime2 regulates meiotic progression in Saccharomyces cerevisiae. J Biol Chem 281, 18307–18316. 10.1074/jbc.M602349200. [PubMed: 16684773]
38. Moore M, Shin ME, Bruning A, Schindler K, Vershon A, and Winter E (2007). Arg-Pro-X-Ser/Thr is a consensus phosphoacceptor sequence for the meiosis-specific Ime2 protein kinase in Saccharomyces cerevisiae. Biochemistry 46, 271–278. 10.1021/bi061858p. [PubMed: 17198398]
39. Pak J, and Segall J (2002). Role of Ndt80, Sum1, and Swe1 as targets of the meiotic recombination checkpoint that control exit from pachytene and spore formation in Saccharomyces cerevisiae. Molecular and cellular biology 22, 6430–6440. 10.1128/MCB.22.18.6430-6440.2002. [PubMed: 12192042]

40. Ahmed NT, Bungard D, Shin ME, Moore M, and Winter E (2009). The Ime2 protein kinase enhances the disassociation of the Sum1 repressor from middle meiotic promoters. Molecular and cellular biology 29, 4352–4362. 10.1128/MCB.00305-09. [PubMed: 19528232]
41. Lo HC, Kunz RC, Chen X, Marullo A, Gygi SP, and Hollingsworth NM (2012). Cdc7-Dbf4 is a gene-specific regulator of meiotic transcription in yeast. Molecular and cellular biology 32, 541–557. 10.1128/MCB.06032-11. [PubMed: 22106412]
42. Aitken A, Collinge DB, van Heusden BP, Isobe T, Roseboom PH, Rosenfeld G, and Soll J (1992). 14-3-3 proteins: a highly conserved, widespread family of eukaryotic proteins. Trends Biochem Sci 17, 498–501. 10.1016/0968-0004(92)90339-b. [PubMed: 1471260]
43. van Heusden GP, Wenzel TJ, Lagendijk EL, de Steensma HY, and van den Berg JA (1992). Characterization of the yeast BMH1 gene encoding a putative protein homologous to mammalian protein kinase II activators and protein kinase C inhibitors. FEBS Lett 302, 145–150. 10.1016/0014-5793(92)80426-h. [PubMed: 1378790]
44. van Hemert MJ, van Heusden GP, and Steensma HY (2001). Yeast 14-3-3 proteins. Yeast 18, 889–895. 10.1002/yea.739. [PubMed: 11447594]
45. Muslin AJ, Tanner JW, Allen PM, and Shaw AS (1996). Interaction of 14-3-3 with signaling proteins is mediated by the recognition of phosphoserine. Cell 84, 889–897. 10.1016/s0092-8674(00)81067-3. [PubMed: 8601312]
46. Yaffe MB, Rittinger K, Volinia S, Caron PR, Aitken A, Leffers H, Gamblin SJ, Smerdon SJ, and Cantley LC (1997). The structural basis for 14-3-3:phosphopeptide binding specificity. Cell 91, 961–971. 10.1016/s0092-8674(00)80487-0. [PubMed: 9428519]
47. Sluchanko NN, and Gusev NB (2017). Moonlighting chaperone-like activity of the universal regulatory 14-3-3 proteins. FEBS J 284, 1279–1295. 10.1111/febs.13986. [PubMed: 27973707]
48. Obsil T, Ghirlando R, Klein DC, Ganguly S, and Dyda F (2001). Crystal structure of the 14-3-3zeta:serotonin N-acetyltransferase complex. a role for scaffolding in enzyme regulation. Cell 105, 257–267. 10.1016/s0092-8674(01)00316-6. [PubMed: 11336675]
49. Chen HK, Fernandez-Funez P, Acevedo SF, Lam YC, Kaytor MD, Fernandez MH, Aitken A, Skoulakis EM, Orr HT, Botas J, and Zoghbi HY (2003). Interaction of Akt-phosphorylated ataxin-1 with 14-3-3 mediates neurodegeneration in spinocerebellar ataxia type 1. Cell 113, 457–468. 10.1016/s0092-8674(03)00349-0. [PubMed: 12757707]
50. Lopez-Girona A, Furnari B, Mondesert O, and Russell P (1999). Nuclear localization of Cdc25 is regulated by DNA damage and a 14-3-3 protein. Nature 397, 172–175. 10.1038/16488. [PubMed: 9923681]
51. Braselmann S, and McCormick F (1995). Bcr and Raf form a complex in vivo via 14-3-3 proteins. EMBO J 14, 4839–4848. [PubMed: 7588613]
52. Kumar R (2018). Differential abundance and transcription of 14-3-3 proteins during vegetative growth and sexual reproduction in budding yeast. Sci Rep 8, 2145. 10.1038/s41598-018-20284-6. [PubMed: 29391437]
53. Slubowski CJ, Paulissen SM, and Huang LS (2014). The GCKIII kinase Sps1 and the 14-3-3 isoforms, Bmh1 and Bmh2, cooperate to ensure proper sporulation in Saccharomyces cerevisiae. PloS one 9, e113528. 10.1371/journal.pone.0113528. [PubMed: 25409301]
54. Luo ZJ, Zhang XF, Rapp U, and Avruch J (1995). Identification of the 14.3.3 zeta domains important for self-association and Raf binding. J Biol Chem 270, 23681–23687. 10.1074/jbc.270.40.23681. [PubMed: 7559537]
55. Liu YC, Elly C, Yoshida H, Bonnefoy-Berard N, and Altman A (1996). Activation-modulated association of 14-3-3 proteins with Cbl in T cells. J Biol Chem 271, 14591–14595. 10.1074/jbc.271.24.14591. [PubMed: 8663231]
56. Ichimura T, Uchiyama J, Kunihiro O, Ito M, Horigome T, Omata S, Shinkai F, Kaji H, and Isobe T (1995). Identification of the site of interaction of the 14-3-3 protein with phosphorylated tryptophan hydroxylase. J Biol Chem 270, 28515–28518. 10.1074/jbc.270.48.28515. [PubMed: 7499362]
57. Wakui H, Wright AP, Gustafsson J, and Zilliacus J (1997). Interaction of the ligand-activated glucocorticoid receptor with the 14-3-3 eta protein. J Biol Chem 272, 8153–8156. 10.1074/jbc.272.13.8153. [PubMed: 9079630]

58. Prugar E, Burnett C, Chen X, and Hollingsworth NM (2017). Coordination of Double Strand Break Repair and Meiotic Progression in Yeast by a Mek1-Ndt80 Negative Feedback Loop. Genetics 206, 497–512. 10.1534/genetics.117.199703. [PubMed: 28249986]
59. Chen X, Gaglione R, Leong T, Bednor L, de Los Santos T, Luk E, Airola M, and Hollingsworth NM (2018). Mek1 coordinates meiotic progression with DNA break repair by directly phosphorylating and inhibiting the yeast pachytene exit regulator Ndt80. PLoS Genet 14, e1007832. 10.1371/journal.pgen.1007832. [PubMed: 30496175]
60. Rockmill B, and Roeder GS (1991). A meiosis-specific protein kinase homolog required for chromosome synapsis and recombination. Genes Dev 5, 2392–2404. 10.1101/gad.5.12b.2392. [PubMed: 1752435]
61. Hollingsworth NM, and Gaglione R (2019). The meiotic-specific Mek1 kinase in budding yeast regulates interhomolog recombination and coordinates meiotic progression with double-strand break repair. Curr Genet 65, 631–641. 10.1007/s00294-019-00937-3. [PubMed: 30671596]
62. Lydall D, Nikolsky Y, Bishop DK, and Weinert T (1996). A meiotic recombination checkpoint controlled by mitotic checkpoint genes. Nature 383, 840–843. 10.1038/383840a0. [PubMed: 8893012]
63. Weinert TA, Kiser GL, and Hartwell LH (1994). Mitotic checkpoint genes in budding yeast and the dependence of mitosis on DNA replication and repair. Genes Dev 8, 652–665. 10.1101/gad.8.6.652. [PubMed: 7926756]
64. Subramanian VV, and Hochwagen A (2014). The meiotic checkpoint network: step-by-step through meiotic prophase. Cold Spring Harb Perspect Biol 6, a016675. 10.1101/cshperspect.a016675. [PubMed: 25274702]
65. Zhao X, Muller EG, and Rothstein R (1998). A suppressor of two essential checkpoint genes identifies a novel protein that negatively affects dNTP pools. Mol Cell 2, 329–340. 10.1016/s1097-2765(00)80277-4. [PubMed: 9774971]
66. Keeney S, Giroux CN, and Kleckner N (1997). Meiosis-specific DNA double-strand breaks are catalyzed by Spo11, a member of a widely conserved protein family. Cell 88, 375–384. 10.1016/s0092-8674(00)81876-0. [PubMed: 9039264]
67. Hollenberg SM, Sternglanz R, Cheng PF, and Weintraub H (1995). Identification of a new family of tissue-specific basic helix-loop-helix proteins with a two-hybrid system. Molecular and cellular biology 15, 3813–3822. 10.1128/MCB.15.7.3813. [PubMed: 7791788]
68. Tung KS, Hong EJ, and Roeder GS (2000). The pachytene checkpoint prevents accumulation and phosphorylation of the meiosis-specific transcription factor Ndt80. Proc Natl Acad Sci U S A 97, 12187–12192. 10.1073/pnas.220464597. [PubMed: 11035815]
69. Carlile TM, and Amon A (2008). Meiosis I is established through division-specific translational control of a cyclin. Cell 133, 280–291. 10.1016/j.cell.2008.02.032. [PubMed: 18423199]
70. Schwab M, Lutum AS, and Seufert W (1997). Yeast Hct1 is a regulator of Clb2 cyclin proteolysis. Cell 90, 683–693. 10.1016/s0092-8674(00)80529-2. [PubMed: 9288748]
71. Visintin R, Prinz S, and Amon A (1997). CDC20 and CDH1: a family of substrate-specific activators of APC-dependent proteolysis. Science 278, 460–463. 10.1126/science.278.5337.460. [PubMed: 9334304]
72. Shirayama M, Zachariae W, Ciosk R, and Nasmyth K (1998). The Polo-like kinase Cdc5p and the WD-repeat protein Cdc20p/fizzy are regulators and substrates of the anaphase promoting complex in Saccharomyces cerevisiae. EMBO J 17, 1336–1349. 10.1093/emboj/17.5.1336. [PubMed: 9482731]
73. Clyne RK, Katis VL, Jessop L, Benjamin KR, Herskowitz I, Lichten M, and Nasmyth K (2003). Polo-like kinase Cdc5 promotes chiasmata formation and cosegregation of sister centromeres at meiosis I. Nature cell biology 5, 480–485. 10.1038/ncb977. [PubMed: 12717442]
74. Lee BH, and Amon A (2003). Role of Polo-like kinase CDC5 in programming meiosis I chromosome segregation. Science 300, 482–486. 10.1126/science.1081846. [PubMed: 12663816]
75. Sourirajan A, and Lichten M (2008). Polo-like kinase Cdc5 drives exit from pachytene during budding yeast meiosis. Genes Dev 22, 2627–2632. 10.1101/gad.1711408. [PubMed: 18832066]

76. Attner MA, Miller MP, Ee LS, Elkin SK, and Amon A (2013). Polo kinase Cdc5 is a central regulator of meiosis I. Proc Natl Acad Sci U S A 110, 14278–14283. 10.1073/pnas.1311845110. [PubMed: 23918381]
77. Snead JL, Sullivan M, Lowery DM, Cohen MS, Zhang C, Randle DH, Taunton J, Yaffe MB, Morgan DO, and Shokat KM (2007). A coupled chemical-genetic and bioinformatic approach to Polo-like kinase pathway exploration. Chem Biol 14, 1261–1272. 10.1016/j.chembiol.2007.09.011. [PubMed: 18022565]
78. Du J, Chen L, Luo X, Shen Y, Dou Z, Shen J, Cheng L, Chen Y, Li C, Wang H, and Yao X (2012). 14-3-3zeta cooperates with phosphorylated Plk1 and is required for correct cytokinesis. Front Biosci (Schol Ed) 4, 639–650. 10.2741/s290. [PubMed: 22202082]
79. van Heusden GP, and Steensma HY (2006). Yeast 14-3-3 proteins. Yeast 23, 159–171. 10.1002/yea.1338. [PubMed: 16498703]
80. van Hemert MJ, Steensma HY, and van Heusden GP (2001). 14-3-3 proteins: key regulators of cell division, signalling and apoptosis. Bioessays 23, 936–946. 10.1002/bies.1134. [PubMed: 11598960]
81. Lee KS, and Erikson RL (1997). Plk is a functional homolog of Saccharomyces cerevisiae Cdc5, and elevated Plk activity induces multiple septation structures. Molecular and cellular biology 17, 3408–3417. 10.1128/MCB.17.6.3408. [PubMed: 9154840]
82. Mohapatra SK, Sandhu A, Neerukattu VS, Singh KP, Selokar NL, Singla SK, Chauhan MS, Manik RS, and Palta P (2015). Buffalo embryos produced by handmade cloning from oocytes selected using brilliant cresyl blue staining have better developmental competence and quality and are closer to embryos produced by in vitro fertilization in terms of their epigenetic status and gene expression pattern. Cell Reprogram 17, 141–150. 10.1089/cell.2014.0077. [PubMed: 25826727]
83. Macurek L, Lindqvist A, Lim D, Lampson MA, Klompmaker R, Freire R, Clouin C, Taylor SS, Yaffe MB, and Medema RH (2008). Polo-like kinase-1 is activated by aurora A to promote checkpoint recovery. Nature 455, 119–123. 10.1038/nature07185. [PubMed: 18615013]
84. Kakiuchi K, Yamauchi Y, Taoka M, Iwago M, Fujita T, Ito T, Song SY, Sakai A, Isobe T, and Ichimura T (2007). Proteomic analysis of in vivo 14-3-3 interactions in the yeast Saccharomyces cerevisiae. Biochemistry 46, 7781–7792. 10.1021/bi700501t. [PubMed: 17559233]
85. Jin L, Zhang K, Sternglanz R, and Neiman AM (2017). Predicted RNA Binding Proteins Pes4 and Mip6 Regulate mRNA Levels, Translation, and Localization during Sporulation in Budding Yeast. Molecular and cellular biology 37. 10.1128/MCB.00408-16.
86. Ballew O, and Lacefield S (2019). The DNA damage checkpoint and the spindle position checkpoint: guardians of meiotic commitment. Curr Genet 65, 1135–1140. 10.1007/s00294-019-00981-z. [PubMed: 31028453]
87. Gihana GM, Musser TR, Thompson O, and Lacefield S (2018). Prolonged cyclin-dependent kinase inhibition results in septin perturbations during return to growth and mitosis. J Cell Biol 217, 2429–2443. 10.1083/jcb.201708153. [PubMed: 29743192]
88. Nachman I, Regev A, and Ramanathan S (2007). Dissecting timing variability in yeast meiosis. Cell 131, 544–556. 10.1016/j.cell.2007.09.044. [PubMed: 17981121]
89. Zaman S, Lippman SI, Zhao X, and Broach JR (2008). How Saccharomyces responds to nutrients. Annu Rev Genet 42, 27–81. 10.1146/annurev.genet.41.110306.130206. [PubMed: 18303986]
90. Janke C, Magiera MM, Rathfelder N, Taxis C, Reber S, Maekawa H, Moreno-Borchart A, Doenges G, Schwob E, Schiebel E, and Knop M (2004). A versatile toolbox for PCR-based tagging of yeast genes: new fluorescent proteins, more markers and promoter substitution cassettes. Yeast 21, 947–962. 10.1002/yea.1142. [PubMed: 15334558]
91. Longtine MS, McKenzie A 3rd, Demarini DJ, Shah NG, Wach A, Brachat A, Philippsen P, and Pringle JR (1998). Additional modules for versatile and economical PCR-based gene deletion and modification in Saccharomyces cerevisiae. Yeast 14, 953–961. 10.1002/(SICI)1097-0061(199807)14:10<953::AID-YEA293>3.0.CO;2-U. [PubMed: 9717241]
92. Gietz RD (2014). Yeast transformation by the LiAc/SS carrier DNA/PEG method. Methods Mol Biol 1205, 1–12. 10.1007/978-1-4939-1363-3_1. [PubMed: 25213235]

93. Wang F, Zhang R, Feng W, Tsuchiya D, Ballew O, Li J, Denic V, and Lacefield S (2020). Autophagy of an Amyloid-like Translational Repressor Regulates Meiotic Exit. Developmental cell 52, 141–151 e145. 10.1016/j.devcel.2019.12.017. [PubMed: 31991104]

Highlights:

- Bcy1, Ime2, Bmh1, Bmh2, Cdc5, and Pes4 are regulators of meiotic commitment
- Bmh1 and Bmh2 bind Ndt80 and maintain Ndt80 levels
- Bmh1/Bmh2 complexes enhance Polo kinase activity for meiotic commitment
- Bmh1 binds RNA-binding protein Pes4

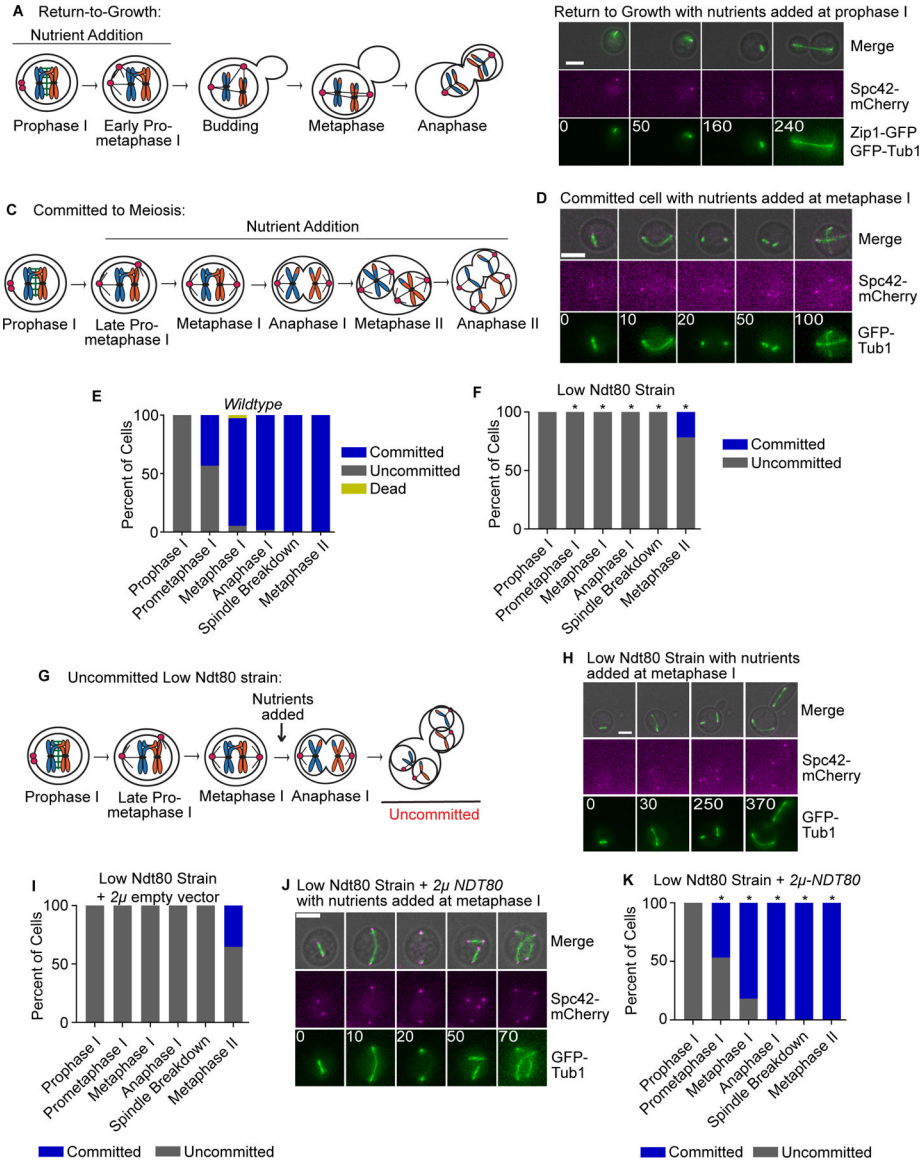

Figure 1: Identification of genes involved in meiotic commitment.

(A) Drawing of a cell undergoing return-to-growth (RTG) upon nutrient addition before early prometaphase I. (B) Time-lapse images of a wildtype cell undergoing RTG upon nutrient addition in pachytene (t = 0). Time in minutes. Scale bar - 5μm. (C) Drawing of a committed cell upon nutrient addition in late prometaphase I - anaphase II. (D) Time-lapse images of a wildtype committed cell upon nutrient addition at metaphase I (t = 0). Time in minutes. Scale bar – 5μm. (E-F) Graph of commitment assay in a (E) wildtype strain (268 cells counted, two experiments) and (F) the low Ndt80 strain (199 cells counted, two experiments). The x-axis shows the stage upon nutrient addition. *denotes a statistically significant difference from wildtype ($p<0.05$, Fisher's exact test). (G) Drawing of an uncommitted low Ndt80 cell upon nutrient addition at metaphase I. (H) Time-lapse images of an uncommitted low Ndt80 cell upon nutrient addition at metaphase I (t = 0). Time in minutes. Scale bar – 5μm. (I) Graph of commitment assay for the low Ndt80 strain

with 2μ-empty vector (256 cells counted, two experiments). The x-axis shows the stage upon nutrient addition. This mutant is not significantly different from the low Ndt80 strain (Fisher's exact test). (J) Time-lapse images of low Ndt80 cell with 2μ-*NDT80* upon nutrient addition at metaphase I (t = 0). Time in minutes. Scale bar – 5μm. (K) Graph of commitment assay for the low Ndt80 + 2μ-*NDT80* (136 cells, two experiments). * denotes a statistically significant difference from Low Ndt80 cells ($p<0.05$, Fisher's exact test). See also Figure S1, Table S1.

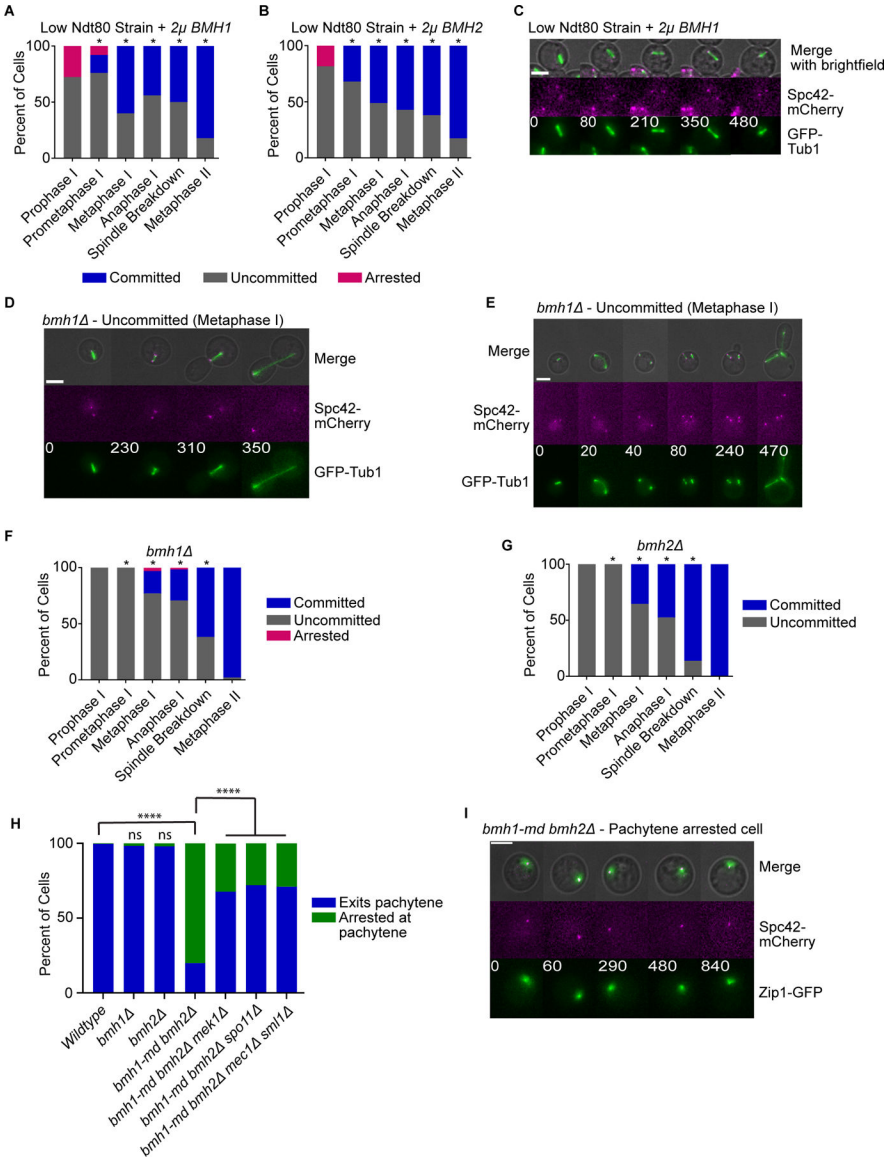

Figure 2: Bmh1 and Bmh2 are important for meiotic commitment and DSB repair.

(A-B) Graph of commitment assay for (A) the low Ndt80 strain with 2μ-*BMH1* (243 cells, two experiments) and (B) the low Ndt80 strain with 2μ-*BMH2* (227 cells, two experiments). The x-axis shows the stage upon nutrient addition. * denotes a statistically significant difference from the low Ndt80 strain ($p<0.05$, Fisher's exact test). (C) Time-lapse images of a committed low Ndt80 + 2μ-*BMH1* cell upon nutrient addition at metaphase I (t = 0). Time in minutes. Scale bar – 5μm. (D and E) Time-lapse images of *bmh1Δ* uncommitted cells upon nutrient addition in metaphase I (t = 0). Time in minutes. Scale bar - 5μm. (F,G) Graph of the commitment assay for (F) the *bmh1Δ* strain (288 cells, three experiments) and (G) *bmh2Δ* strain (363 cells, three experiments). The x-axis shows the stage upon nutrient addition. *denotes a statistically significant difference from wildtype cells ($p<0.05$, Fisher's exact test). (H) Graph of the progression through pachytene for indicated strains (300 cells, three experiments per genotype). ****denotes statistically significant differences ($p<0.0001$,

Fisher's exact test), ns is not significant. (I) Time-lapse images of a *bmh1-md bmh2Δ* cell arrested at pachytene (t = 0 at 8hrs after SPM transfer). Time in minutes. Scale bar - 5μm. See also Figure S2.

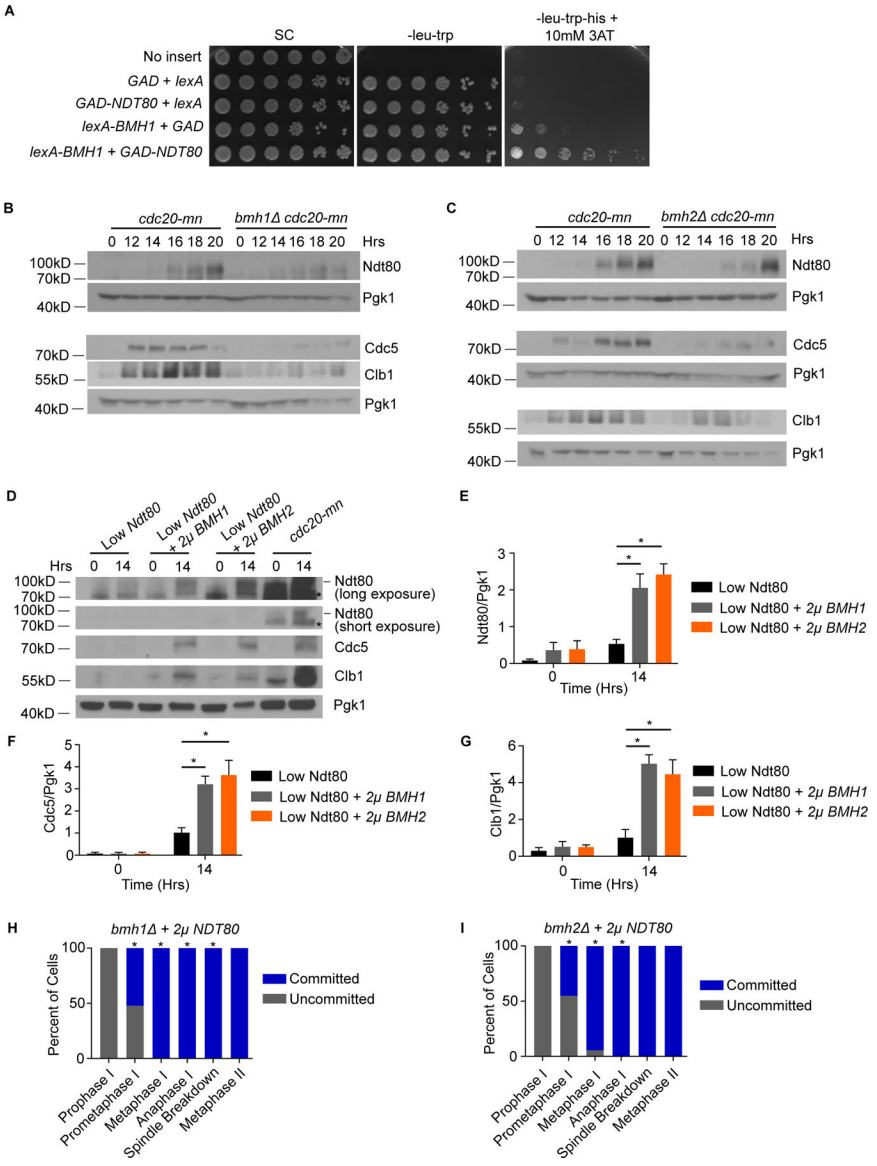

Figure 3: Bmh1 and Bmh2 regulate Ndt80 levels.

(A) Two-hybrid interactions in strains with combinations of *GAL4* activation domain (GAD) and *lexA* DNA-binding domain fused to either *NDT80* (amino acids 287–627) or *BMH1*, with *HIS3* reporter under control of promoter with *lexA* operator sites, and assayed for *HIS3* expression in the presence of 10mM 3-Aminotriazole (3AT) with 10-fold serial dilutions. (B -D) Western blot of Ndt80, Cdc5, Clb1, and Pgk1(loading control) in the indicated strains (t=0 indicates time transferred to SPM). Two western blots in (B) and three western blots in (C). *denotes non-specific band not included in quantification. (E-G) Graphs showing mean ± SEM of the densitometric quantification of Ndt80 (E), Cdc5 (F) and Clb1 (G) levels relative to Pgk1 in the indicated strains and time points (three experiments). *denotes statistically significant difference ($p<0.05$, Unpaired t-test with Welch's correction). (H-I) Graph of the commitment assay for (H) *bmh1Δ* + 2μ-*NDT80* (233 cells, two experiments) and (I) *bmh2Δ* + 2μ-*NDT80* strain (246 cells, two experiments). The x-axis shows stage

upon nutrient addition. *denotes statistically significant difference from (H) *bmh1Δ* cells and (I) *bmh2Δ* cells ($p<0.05$, Fisher's exact test). See also Figure S3.

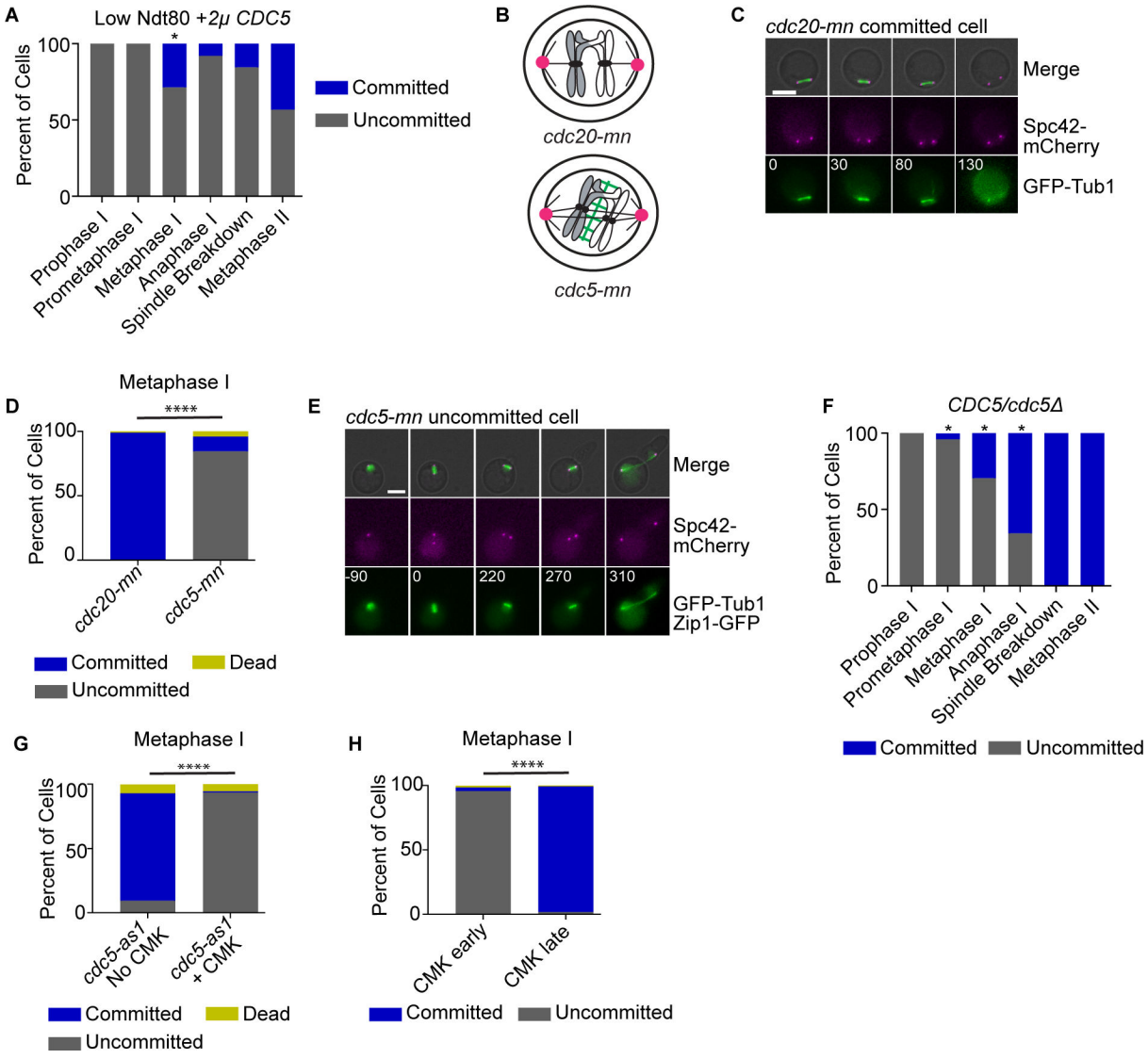

Figure 4: Cdc5 is important for meiotic commitment.

(A) Graph of the commitment assay for low Ndt80 +2μ-*CDC5* strain (202 cells counted, two experiments). *denotes statistically significant difference from the low Ndt80 strain ($p<0.05$, Fisher's exact test). (B) Drawing of *cdc20-mn* and *cdc5-mn* cells arrested in metaphase I. (C) Time-lapse images of a committed *cdc20-mn* cell with nutrient addition at metaphase I (t = 0). Time in minutes. Scale bar - 5μm. (D) Graph of the commitment assay for *cdc20-mn* (n = 113 cells; two experiments) and *cdc5-mn* strains (n = 156; three experiments) with nutrient addition at metaphase I. ****denotes statistically significant difference ($p<0.0001$, Fisher's exact test). (E) Time-lapse images of a *cdc5-mn* uncommitted cell with nutrient addition at metaphase I (t = 0). Time in minutes. Scale bar - 5μm. (F) Graph of commitment assay for *CDC5/cdc5Δ* strain (207 cells, two experiments). The x-axis shows stage upon nutrient addition. *denotes statistically significant difference from wildtype ($p<0.05$, Fisher's exact test). (G) Graph of the commitment assay for *cdc5-as1* strain with CMK inhibitor (n = 108 cells, three experiments) and without inhibitor (n = 42 cells, three experiments) with nutrient addition at metaphase I (t = 0). ****denotes statistically significant difference ($p<0.0001$,

Fisher's exact test). (H) Graph of commitment assay the *cdc5-as1 cdc20-mn* strain with CMK inhibitor added early (pachytene, n = 140 cells, one experiment) and late (metaphase I, n = 168 cells, three experiments) with nutrient addition in metaphase I. ****denotes statistically significant difference ($p<0.0001$, Fisher's exact test).

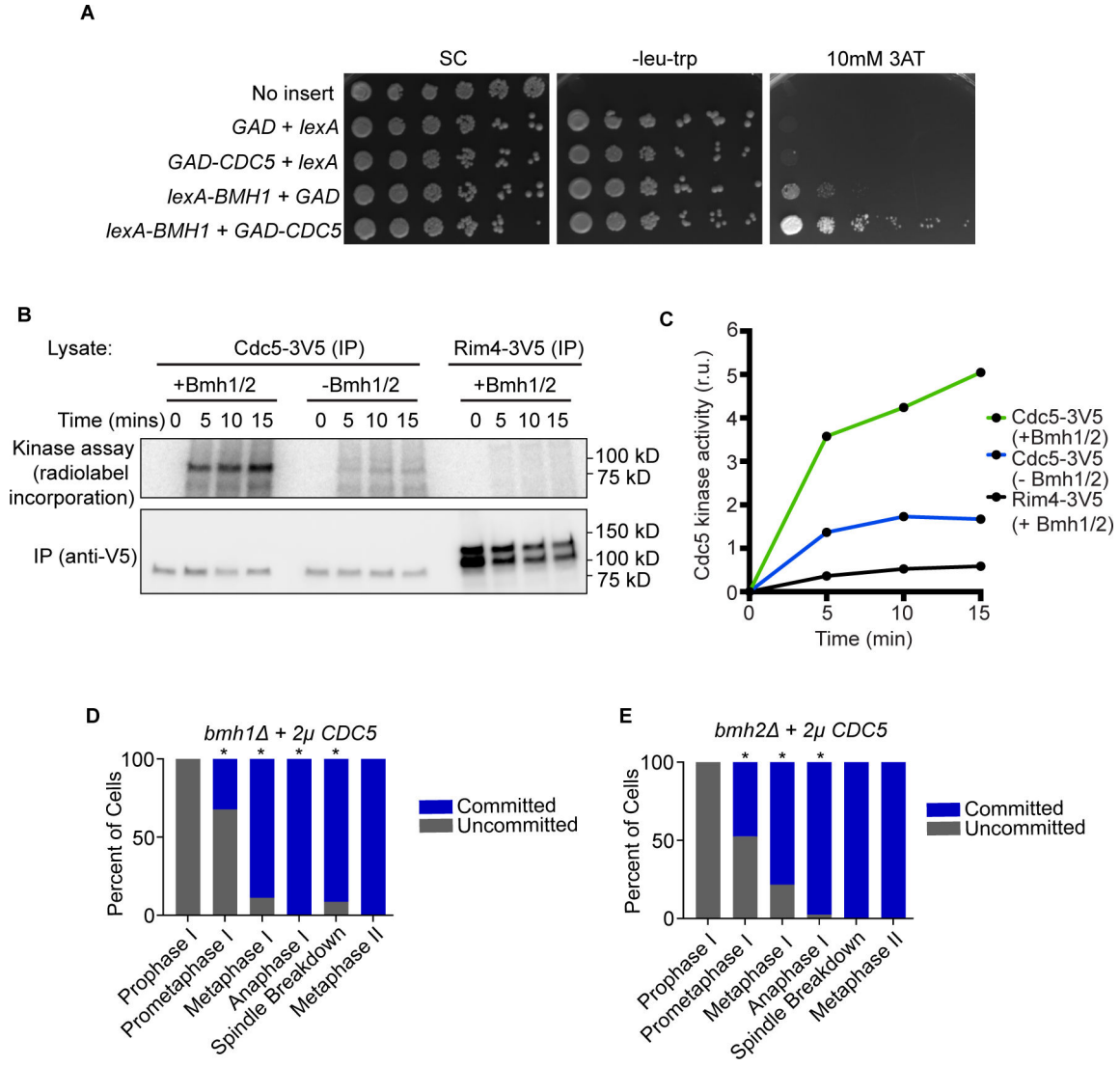

Figure 5: Bmh1/Bmh2 enhances Cdc5 kinase activity.

(A) Two-hybrid interactions in strains with combinations of *GAL4* activation domain (GAD) and *lexA* DNA-binding domain fused to either *CDC5* or *BMH1*, with *HIS3* reporter under control of promoter with *lexA* operator sites, and assayed for *HIS3* expression in the presence of 10mM 3-Aminotriazole (3AT) with 10-fold serial dilutions. (B) Kinase activity assay with immunoprecipitated Cdc5–3V5 or Rim4–3V5 (as a control) +/− purified Bmh1/2 complexes as indicated. Incorporation of radiolabeled ATP assessed at indicated times (upper). Immunoprecipitated Cdc5 and Rim4 are shown with anti-V5 immunoblot (lower). (C) Graph depicting radiolabeled ATP incorporation at indicated timepoints. (D-E) Graph of commitment assay for (D) *bmh1Δ* + 2μ-*CDC5* (222 cells, two experiments) and (E) *bmh2Δ* + 2μ-*CDC5* (175 cells, two experiments). The x-axis shows stage upon nutrient addition. *denotes statistically significant difference from *bmh1Δ* (D) and *bmh2Δ* (E) cells ($p<0.05$, Fisher's exact test). See also Figure S2.

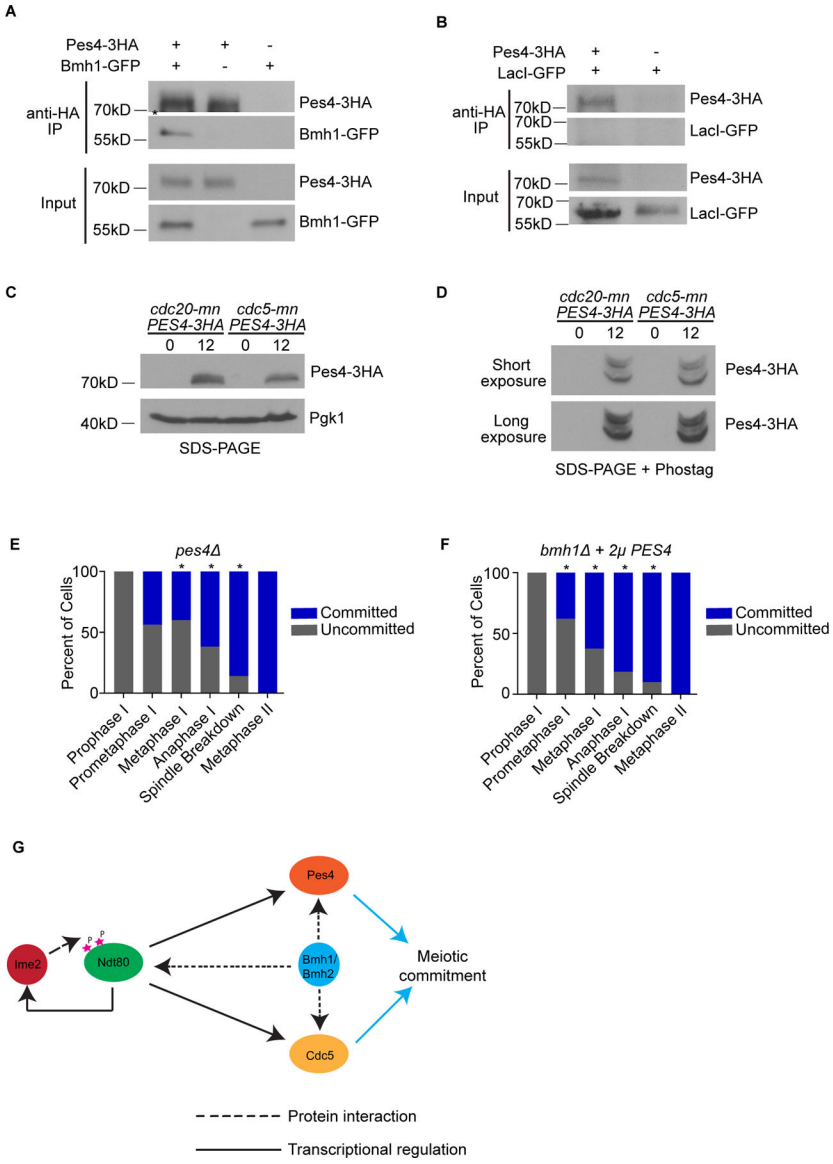

Figure 6: Pes4 binds Bmh1 and is required for meiotic commitment.

(A) Anti-HA immunoprecipitation and immunoblot probing with anti-HA or anti-GFP, as indicated. *PES4–3HA BMH1-GFP* cells were compared to *PES4–3HA* and *BMH1-GFP* cells. Input refers to the extract before immunoprecipitation. *denotes partial IgG band below. (B) Control anti-HA immunoprecipiation and immunoblot with either anti-HA or anti-GFP, as indicated. *PES4–3HA LacI-GFP* cells were compared to *LacI-GFP* cells. (C) Immunoblot of Pes4–3HA levels in *cdc20mn* and *cdc5mn* cells. Time zero indicates time transferred to SPM. Pgk1 is the loading control. (D) Pes4–3HA analyzed on a Phostag gel. Time zero indicates the time transferred to SPM. (E,F) Graph of the commitment assay for (E) *pes4Δ* (186 cells, two experiments) and (F) *bmh1Δ* + 2μ-*PES4* (81 cells, two experiments). The x-axis shows stage at nutrient addition. *denotes statistically significant difference from wildtype (E) and *bmh1Δ* (F) cells ($p<0.05$, Fisher's exact test). (G) Model for meiotic commitment. At prophase I exit, Ime2 phosphorylates and activates

Ndt80. Ndt80 then induces *CDC5*, *PES4* and additional *IME2* expression. Bmh1 interacts with Ndt80, Cdc5 and Pes4. Bmh1 stabilizes Ndt80, enhances Cdc5 kinase activity, and modulates Pes4 to maintain meiotic commitment. See also Figure S2, Table S2.

KEY RESOURCES TABLE

REAGENT or RESOURCE	SOURCE	IDENTIFIER
Antibodies		
anti-Ndt80 rabbit (1:10000)	Gift from Dr. M. Lichten	N/A
Monoclonal anti-Pgk1 mouse (1:10000)	Thermo Fisher Scientific	Cat#459250; RRID: AB_2532235
Polyclonal anti-Cdc5 goat (1:1000)	Santa Cruz Biotechnology	Cat#sc-6733; RRID: AB_671816
Polyclonal anti-Clb1 goat (1:1000)	Santa Cruz Biotechnology	Cat#sc-7647; RRID: AB_671839
Monoclonal anti-HA mouse (1:1000)	Sigma-Aldrich	Cat#11583816001; RRID:AB_514505
ECL-anti-rabbit HRP IgG (1:10000)	GE Healthcare	Cat#NA9340V
ECL-anti-mouse HRP IgG (1:10000)	GE Healthcare	Cat#NA9310V
anti-goat IgG HRP (1:5000)	R&D Systems	Cat#HAF109; RRID: AB_357236
Monoclonal anti-GFP mouse (IP antibody)	Roche	Cat#11814460001; RRID:AB_390913
anti-GFP rabbit (1:10000)	Gift from Dr. C. Walczak	N/A
Anti-V5 Agarose Affinity Gel antibody	Sigma	Cat#A7345
V5 Tag Monoclonal mouse antibody	Invitrogen	Cat#R96025
Chemicals, peptides, and recombinant proteins		
Bacto Peptone	BD Biosciences	Cat#211820
Bacto Yeast Extract	BD Biosciences	Cat#212720
Yeast Nitrogen Bases without amino acids	Difco Laboraties	Cat#291920
Glucose/Dextrose	Fisher BioReagents	Cat#D16–10
Potassium Acetate	Fisher BioReagents	Cat#P171–500
Chloromethylketone	Gift from Dr. A Marston	N/A
Trichloroacetic acid	Sigma	Cat#76–03–9
Tris-HCl	Sigma	Cat#76–03–9
EDTA	Sigma	Cat#6381–92–6
DTT	Bio-Rad	Cat#161–0611
Pierce Protease Inhibitor Mini tablet-EDTA free	Thermo Fisher Scientific	Cat#A32955
Sodium Dodecyl Sulfate	Bio-Rad	Cat#1610301
Phos-tag™	Fujifilm	Cat#AAL107
Manganese chloride	Sigma	Cat#13220
Tween 20	Sigma	Cat#9005–64–5
3-aminotriazole	Sigma	Cat#A8056
Sodium Chloride	EMD	Cat#7647–14–5
Magnesium chloride	Sigma	Cat#8266

REAGENT or RESOURCE	SOURCE	IDENTIFIER
Glycerol	VWR Chemicals	Cat#56–81–5
NP-40	Sigma	Cat#492016
DYNAbeads Protein G	Invitrogen	Cat#10003D
4–20% Mini-PROTEAN TGX Precast protein gel	BIO-RAD	Cat#4561094
Imperial Protein Stain	Thermo Fisher	Cat#24615
Tris (2-carboxyethyl) phosphine hydrochloride	Sigma	Cat#C4706
Iodoacetamide	Sigma	Cat#I6125
Trypsin	Promega	Cat#V5113
Halt protease and phosphatase inhibitor cocktail	Thermo	Cat#78441
2-Mercaptoethanol	Sigma	Cat#M3148
Copper Sulfate	Sigma	Cat#7758–99–8
Radiolabeled ATP (gamma-labeled) ATP, [γ-32P]- 3000Ci/mmol 10mCi/ml EasyTide, 250 μCi	PerkinElmer	Cat#BLU502A250UC
Critical commercial assays		
Pierce Coomassie Plus Assay kit	Thermo Scientific	Cat#23236
Experimental models: Organisms/strains		
MATa/α, P_{TUB1}-GFP-TUB1:LEU2/ P_{TUB1}-GFP-TUB1:LEU2, ZIP1-GFP/+, SPC42-mCherry:kanMX/+	Lacefield Lab	LY4027
MATa/α, P_{TUB1}-GFP-TUB1:URA3/+, ZIP1-GFP/+, SPC42-mCherry:kanMX/+, ndt80::kanMX/ ndt80::kanMX, $P_{NDT80\text{-}mse1\Delta,\ mse1\Delta}$ NDT80:HIS3/ $P_{NDT80\text{-}mse1\Delta,\ mse1\Delta}$ NDT80:HIS3, ADE2/ADE2, TRP1/TRP1	Lacefield Lab	LY4273
MATa/α, P_{TUB1}-GFP-TUB1:URA3/+, ZIP1-GFP/+, SPC42-mCherry:kanMX/+, ndt80::kanMX/ ndt80::kanMX, $P_{NDT80\text{-}mse1\Delta,\ mse1\Delta}$ NDT80:HIS3/ $P_{NDT80\text{-}mse1\Delta,\ mse1\Delta}$ NDT80:HIS3, ADE2/ADE2, TRP1/TRP1, pLB227 (2μ)	Lacefield Lab	LY4404
MATa/α, P_{TUB1}-GFP-TUB1:URA3/+, ZIP1-GFP/+, SPC42-mCherry:kanMX/+, ndt80::kanMX/ ndt80::kanMX, $P_{NDT80\text{-}mse1\Delta,\ mse1\Delta}$ NDT80:HIS3/ $P_{NDT80\text{-}mse1\Delta,\ mse1\Delta}$ NDT80:HIS3, ADE2/ADE2, TRP1/TRP1, P_{NDT80}-NDT80:LEU2 (2μ)	Lacefield Lab	LY4285
MATa/α, P_{TUB1}-GFP-TUB1:URA3/+, ZIP1-GFP/+, SPC42-mCherry:kanMX/+, ndt80::kanMX/ ndt80::kanMX, $P_{NDT80\text{-}mse1\Delta,\ mse1\Delta}$ NDT80:HIS3/ $P_{NDT80\text{-}mse1\Delta,\ mse1\Delta}$ NDT80:HIS3, ADE2/ADE2, TRP1/TRP1, P_{BCY1}-BCY1:LEU2 (2μ)	Lacefield Lab	LY5463
MATa/α, P_{TUB1}-GFP-TUB1:LEU2/ P_{TUB1}-GFP-TUB1:LEU2, ZIP1-GFP/+, SPC42-mCherry:kanMX/+, bcy1::NAT/+	Lacefield Lab	LY8715
MATa/α, P_{TUB1}-GFP-TUB1:URA3/+, ZIP1-GFP/+, SPC42-mCherry:kanMX/+, ndt80::kanMX/ ndt80::kanMX, $P_{NDT80\text{-}mse1\Delta,\ mse1\Delta}$ NDT80:HIS3/ $P_{NDT80\text{-}mse1\Delta,\ mse1\Delta}$ NDT80:HIS3, ADE2/ADE2, TRP1/TRP1, P_{IME2}-IME2:LEU2 (2μ)	Lacefield Lab	LY5465
MATa/α, P_{TUB1}-GFP-TUB1:URA3/ P_{TUB1}-GFP-TUB1:URA3, ZIP1-GFP/+, SPC42-mCherry:HPH/+, ime2::HPH/ ime2::HPH, P_{IME2}-IME2-myc-TRP1:TRP1/ P_{IME2}-IME2-myc-TRP1:TRP1, sum1::kanMX/sum1::NAT	Lacefield Lab	LY8932
MATa/α, P_{TUB1}-GFP-TUB1:URA3/ P_{TUB1}-GFP-TUB1:URA3, ZIP1-GFP/+, SPC42-mCherry:HPH/+, ime2::HPH/ ime2::HPH, P_{IME2}-IME2 T242A-myc-TRP1:TRP1/ P_{IME2}-IME2 T242A-myc-TRP1:TRP1, sum1::kanMX/sum1::kanMX	Lacefield Lab	LY5694
MATa/α, P_{TUB1}-GFP-TUB1:URA3/+, ZIP1-GFP/+, SPC42-mCherry:kanMX/+, ndt80::kanMX/ ndt80::kanMX, $P_{NDT80\text{-}mse1\Delta,\ mse1\Delta}$ NDT80:HIS3/ P	Lacefield Lab	LY5584

REAGENT or RESOURCE	SOURCE	IDENTIFIER
$_{NDT80\text{-}mse1\Delta,\ mse1\Delta}$ NDT80:HIS3, ADE2/ADE2, TRP1/TRP1, P $_{BMH1}$ -BMH1:LEU2 (2μ)		
MATa/α, P $_{TUB1}$ -GFP-TUB1:URA3/+, ZIP1-GFP/+, SPC42-mCherry:kanMX/+, ndt80::kanMX/ ndt80::kanMX, P $_{NDT80\text{-}mse1\Delta,\ mse1\Delta}$ NDT80:HIS3/ P $_{NDT80\text{-}mse1\Delta,\ mse1\Delta}$ NDT80:HIS3, ADE2/ADE2, TRP1/TRP1, P $_{BMH2}$ -BMH2:LEU2 (2μ)	Lacefield Lab	LY8279
MATa/α, P $_{TUB1}$ -GFP-TUB1:LEU2/ P $_{TUB1}$ -GFP-TUB1:LEU2, ZIP1-GFP/+, SPC42-mCherry:kanMX/+, bmh1::NAT/bmh1::NAT	Lacefield Lab	LY5663
MATa/α, P $_{TUB1}$ -GFP-TUB1:LEU2/ P $_{TUB1}$ -GFP-TUB1:LEU2, ZIP1-GFP/+, SPC42-mCherry:kanMX/+, bmh2::NAT/bmh2::NAT	Lacefield Lab	LY5837
MATa/α, P $_{TUB1}$ -GFP-TUB1:LEU2/ P $_{TUB1}$ -GFP-TUB1:LEU2, ZIP1-GFP/+, SPC42-mCherry:hphMX/+, bmh2::NAT/bmh2::NAT, kanMX:P $_{CLB2}$ -BMH1/ kanMX:P $_{CLB2}$ -BMH1	Lacefield Lab	LY6884
MATa/α, P $_{TUB1}$ -GFP-TUB1:LEU2/ P $_{TUB1}$ -GFP-TUB1:LEU2, ZIP1-GFP/+, SPC42-mCherry:hphMX/+, bmh2::NAT/bmh2::NAT, kanMX:P $_{CLB2}$ -BMH1/ kanMX:P $_{CLB2}$ -BMH1, mek1::HIS3/mek1::HIS3	Lacefield Lab	LY6948
MATa/α, P $_{TUB1}$ -GFP-TUB1:LEU2/ P $_{TUB1}$ -GFP-TUB1:LEU2, ZIP1-GFP/+, SPC42-mCherry:hphMX/+, bmh2::NAT/bmh2::NAT, kanMX:P $_{CLB2}$ -BMH1/ kanMX:P $_{CLB2}$ -BMH1, spo11::HIS3/spo11::HIS3	Lacefield Lab	LY6963
MATa/α, P $_{TUB1}$ -GFP-TUB1:LEU2/ P $_{TUB1}$ -GFP-TUB1:LEU2, ZIP1-GFP/+, SPC42-mCherry:hphMX/+, bmh2::NAT/bmh2::NAT, kanMX:P $_{CLB2}$ -BMH1/ kanMX:P $_{CLB2}$ -BMH1, mec1::LEU2/mec1::LEU2, sml1Δ/sml1Δ	Lacefield Lab	LY6981
MATa/α, P $_{TUB1}$ -GFP-TUB1:URA3/ P $_{TUB1}$ -GFP-TUB1:URA3, ZIP1-GFP/+, SPC42-mCherry:kanMX/+, cdc20::P $_{CLB2}$ -3HA-CDC20::kanMX6/ cdc20::P $_{CLB2}$ -3HA-CDC20::kanMX6	Lacefield Lab	LY6257
MATa/α, P $_{TUB1}$ -GFP-TUB1:URA3/ P $_{TUB1}$ -GFP-TUB1:URA3, ZIP1-GFP/+, SPC42-mCherry:kanMX/+, cdc20::P $_{CLB2}$ -3HA-CDC20::kanMX6/ cdc20::P $_{CLB2}$ -3HA-CDC20::kanMX6, bmh1::HPH/bmh1::HPH	Lacefield Lab	LY6250
MATa/α, P $_{TUB1}$ -GFP-TUB1:URA3/ P $_{TUB1}$ -GFP-TUB1:URA3, ZIP1-GFP/+, SPC42-mCherry:kanMX/+, cdc20::P $_{CLB2}$ -3HA-CDC20::kanMX6/ cdc20::P $_{CLB2}$ -3HA-CDC20::kanMX6, bmh2::HPH/bmh2::HPH	Lacefield Lab	LY6284
MATa/α, P $_{TUB1}$ -GFP-TUB1:LEU2/ P $_{TUB1}$ -GFP-TUB1:LEU2, ZIP1-GFP/+, SPC42-mCherry:kanMX/+, bmh1::NAT/bmh1::NAT, P $_{NDT80}$ -NDT80:URA3 (2μ)	Lacefield Lab	LY7903
MATa/α, P $_{TUB1}$ -GFP-TUB1:LEU2/ P $_{TUB1}$ -GFP-TUB1:LEU2, ZIP1-GFP/+, SPC42-mCherry:kanMX/+, bmh2::NAT/bmh2::NAT, P $_{NDT80}$ -NDT80:URA3 (2μ)	Lacefield Lab	LY7905
MATa/α, P $_{TUB1}$ -GFP-TUB1:URA3/ P $_{TUB1}$ -GFP-TUB1:URA3, ZIP1-GFP/+, SPC42-mCherry:kanMX/+, cdc20::P $_{CLB2}$ -3HA-CDC20::kanMX6/ cdc20::P $_{CLB2}$ -3HA-CDC20::kanMX6	Lacefield Lab	LY3273
MATa/α, P $_{TUB1}$ -GFP-TUB1:URA3/ P $_{TUB1}$ -GFP-TUB1:URA3, ZIP1-GFP/+, SPC42-mCherry:kanMX/+, kanMX:P $_{CLB2}$ -CDC5/ kanMX:P $_{CLB2}$ -CDC5	Lacefield Lab	LY2289
MATa/α, P $_{TUB1}$ -GFP-TUB1:URA3/ P $_{TUB1}$ -GFP-TUB1:URA3, ZIP1-GFP/+, SPC42-mCherry:HPH/+, cdc5::NAT/+	Lacefield Lab	LY3515
MATa/α, P $_{TUB1}$ -GFP-TUB1:URA3/ P $_{TUB1}$ -GFP-TUB1:URA3, ZIP1-GFP/+, SPC42-mCherry:HPH/+, cdc5L158G:NAT/ cdc5L158G:NAT	Lacefield Lab	LY3518
MATa/α, P $_{TUB1}$ -GFP-TUB1:URA3/ P $_{TUB1}$ -GFP-TUB1:URA3, ZIP1-GFP/+, SPC42-mCherry:HPH/+, cdc5L158G:NAT/ cdc5L158G:NAT, cdc20::P $_{CLB2}$ -3HA-CDC20::kanMX6/ cdc20::P $_{CLB2}$ -3HA-CDC20::kanMX6	Lacefield Lab	LY3639
SEY6210 MATa, his3Δ200 trp1–90 leu2–3,112 ade2 gal80 lys2::lexA $_{op}$ -HIS3::LYS2 ura3:: lexA $_{op}$ -lacZ::URA3	Gift from Hollingsworth Lab	LY8522

REAGENT or RESOURCE	SOURCE	IDENTIFIER
SEY6210 MATa, his3Δ200 trp1–90 leu2–3,112 ade2 gal80 lys2::lexA $_{op}$ -HIS3::LYS2 ura3:: lexA $_{op}$ -lacZ::URA3, GAL4AD-NDT80(284–627):LEU2 (2μ), lexA:TRP1 (2μ)	Lacefield Lab	LY8770
SEY6210 MATa, his3Δ200 trp1–90 leu2–3,112 ade2 gal80 lys2::lexA $_{op}$ -HIS3::LYS2 ura3:: lexA $_{op}$ -lacZ::URA3, GAL4AD-NDT80(284–627):LEU2 (2μ), lexA-BMH1:TRP1 (2μ)	Lacefield Lab	LY8772
SEY6210 MATa, his3Δ200 trp1–90 leu2–3,112 ade2 gal80 lys2::lexA $_{op}$ -HIS3::LYS2 ura3:: lexA $_{op}$ -lacZ::URA3, GAL4AD:LEU2 (2μ), lexA:TRP1 (2μ)	Lacefield Lab	LY8767
SEY6210 MATa, his3Δ200 trp1–90 leu2–3,112 ade2 gal80 lys2::lexA $_{op}$ -HIS3::LYS2 ura3:: lexA $_{op}$ -lacZ::URA3, GAL4AD-CDC5:LEU2 (2μ), lexA:TRP1 (2μ)	Lacefield Lab	LY8768
SEY6210 MATa, his3Δ200 trp1–90 leu2–3,112 ade2 gal80 lys2::lexA $_{op}$ -HIS3::LYS2 ura3:: lexA $_{op}$ -lacZ::URA3, GAL4AD:LEU2 (2μ), lexA-BMH1:TRP1 (2μ)	Lacefield Lab	LY8769
SEY6210 MATa, his3Δ200 trp1–90 leu2–3,112 ade2 gal80 lys2::lexA $_{op}$ -HIS3::LYS2 ura3:: lexA $_{op}$ -lacZ::URA3, GAL4AD-CDC5:LEU2 (2μ), lexA-BMH1:TRP1 (2μ)	Lacefield Lab	LY8771
MATa/α, P $_{TUB1}$ -GFP-TUB1:LEU2/ P $_{TUB1}$ -GFP-TUB1:LEU2, ZIP1-GFP/+, SPC42-mCherry:kanMX/+, bmh1::NAT/bmh1::NAT, P $_{CDC5}$ -CDC5:URA3 (2μ)	Lacefield Lab	LY7771
MATa/α, P $_{TUB1}$ -GFP-TUB1:LEU2/ P $_{TUB1}$ -GFP-TUB1:LEU2, ZIP1-GFP/+, SPC42-mCherry:kanMX/+, bmh2::NAT/bmh2::NAT, P $_{CDC5}$ -CDC5:URA3 (2μ)	Lacefield Lab	LY7790
MATa/α, P $_{TUB1}$ -GFP-TUB1:LEU2/ P $_{TUB1}$ -GFP-TUB1:LEU2, ZIP1-GFP/+, SPC42-mCherry:kanMX/+, bmh1::NAT/bmh1::NAT, P $_{BMH1}$ -BMH1 3A:HIS3/ P $_{BMH1}$ -BMH1 3A:HIS3 (at BMH1 locus)	Lacefield Lab	LY8780
MATa/α, P $_{TUB1}$ -GFP-TUB1:LEU2/ P $_{TUB1}$ -GFP-TUB1:LEU2, ZIP1-GFP/+, SPC42-mCherry:kanMX/+, pes4::NAT/pes4::NAT	Lacefield Lab	LY8592
MATa/α, P $_{TUB1}$ -GFP-TUB1:LEU2/ P $_{TUB1}$ -GFP-TUB1:LEU2, ZIP1-GFP/+, SPC42-mCherry:kanMX/+, bmh1::NAT/bmh1::NAT, P $_{PES4}$ -PES4:URA3 (2μ)	Lacefield Lab	LY8934
MATa/α, SPC42-mCherry:HPH/+, BMH1-EGFP:HIS5/ BMH1-EGFP:HIS5	Lacefield Lab	LY8489
MATa/α, SPC42-mCherry:kanMX/+	Lacefield Lab	LY2906
SK1 MATa ho::LYS2 lys2 ura3 leu2::hisG his3::hisG trp1::hisG	Berchowitz Lab	B1421
SK1 MATa ho::LYS2 lys2 ura3 leu2::hisG his3::hisG trp1::hisG CDC5–3V5::G418R	Berchowitz Lab	B2424
SK1 MATa/α ho::LYS2/ho::LYS2 lys2/lys2 ura3/ura3 leu2::hisG/leu2::hisG his3::hisG/his3::hisG trp1::hisG/trp1::hisG ura3::P $_{GPD1}$ -GAL4(848).ER::URA3/ ura3::P $_{GPD1}$ -GAL4(848).ER::URA3 P $_{GAL}$ -NDT80::TRP1/P $_{GAL}$ -NDT80::TRP1 CLB3–3HA:KanR/CLB3–3HA:KanR RIM4–3V5::HIS3/RIM4–3V5::HIS3	Berchowitz Lab	B48
MATa/α, P $_{TUB1}$ -GFP-TUB1:URA3/ P $_{TUB1}$ -GFP-TUB1:URA3, ZIP1-GFP/+, SPC42-mCherry:kanMX/+, cdc20::P $_{CLB2}$ -3HA-CDC20::kanMX6/ cdc20::P $_{CLB2}$ -3HA-CDC20::kanMX6, P $_{PES4}$:PES4:3HA:TRP1/ P $_{PES4}$:PES4:3HA:TRP1	Lacefield Lab	LY9023
MATa/α, P $_{TUB1}$ -GFP-TUB1:URA3/ P $_{TUB1}$ -GFP-TUB1:URA3, ZIP1-GFP/+, SPC42-mCherry:kanMX/+, kanMX:P $_{CLB2}$ -CDC5/ kanMX:P $_{CLB2}$ -CDC5, P $_{PES4}$:PES4:3HA:TRP1/ P $_{PES4}$:PES4:3HA:TRP1	Lacefield Lab	LY9024
MATa/α, SPC42-mCherry:HPH/+, BMH1-EGFP:HIS5/ BMH1-EGFP:HIS5, PES4–3HA:TRP1/PES4–3HA:TRP1	Lacefield Lab	LY8739
MATa/α, SPC42-mCherry:HPH/+, PES4–3HA:TRP1/PES4–3HA:TRP1	Lacefield Lab	LY9308
MATa/α, SPC42-mCherry:HPH/+, PES4–3HA:TRP1/ PES4–3HA:TRP1, cup1pr-LacI-GFP:HIS3/cup1pr-LacI-GFP:HIS3	Lacefield Lab	LY9312
MATa/α, cup1pr-LacI-GFP:HIS3/cup1pr-LacI-GFP:HIS3	Lacefield Lab	LY9300

REAGENT or RESOURCE	SOURCE	IDENTIFIER
MATa/α, P $_{TUB1}$ -GFP-TUB1:URA3/ P $_{TUB1}$ -GFP-TUB1:URA3, ZIP1-GFP/+, SPC42-mCherry:kanMX/+, P $_{BMH1}$ -BMH1:LEU2 (2μ)	Lacefield Lab	LY9310
MATa/α, P $_{TUB1}$ -GFP-TUB1:URA3/ P $_{TUB1}$ -GFP-TUB1:URA3, ZIP1-GFP/+, SPC42-mCherry:kanMX/+, ime2::HPH/ ime2::HPH, P $_{IME2}$ -IME2 T242A-myc-TRP1:TRP1/ P $_{IME2}$ -IME2 T242A-myc-TRP1:TRP1	Lacefield Lab	LY5430
Oligonucleotides		
See Table S3		
Recombinant DNA		
URA3 (2μ)	[92]	YEplac195
LEU2 (2μ)	[92]	YEplac181
3HA:TRP1	[90]	YM22
lexA:TRP1 (2μ)	[59]	pBTM116
GAL4AD:LEU2 (2μ)	[59]	pACTII
Empty vector for the screen	This study	pLB227
P $_{NDT80}$ -NDT80:LEU2 (2μ)	This study	pLB225
P $_{BMH1}$ -BMH1:LEU2 (2μ)	This study	pLB262
P $_{BMH2}$ -BMH2:LEU2 (2μ)	This study	pLB539
lexA-BMH1:TRP1 (2μ)	This study	pLB518
GAL4AD-CDC5:LEU2 (2μ)	This study	pLB491
P $_{CDC5}$ -CDC5:LEU2 (2μ)	This study	pLB463
P $_{CDC5}$ -CDC5:URA3 (2μ)	This study	pLB465
P $_{BMH1}$ -BMH1:HIS3	This study	pLB509
P $_{BMH1}$ -BMH1 3A:HIS3	This study	pLB519
P $_{PES4}$ -PES4:URA3 (2μ)	This study	pLB513
P $_{BCY1}$ -BCY1:LEU2 (2μ)	This study	pLB306
P $_{IME2}$ -IME2:LEU2 (2μ)	This study	pLB258
P $_{IME2}$ -IME2-myc-TRP1	This study	pLB268
P $_{IME2}$ -IME2 T242A-myc-TRP1	This study	pLB285
P $_{NDT80}$ -NDT80:HIS3	This study	pLB107
Yeast Genome Tiling Collection	[28]	N/A
Software and algorithms		
FIJI (ImageJ)	National Institutes of Health (Public Domain)	https://imagej.nih.gov/ij
NIS Elements Viewer v4.20.00 (Build972) LO, 32 bit	Nikon	https://www.nikoninstruments.com/Products/Software/NIS-Elements-Advanced-Research/NISElements-Viewer

REAGENT or RESOURCE	SOURCE	IDENTIFIER
GraphPad Prism 7.03	GraphPad Software, Inc	https://www.graphpad.com/
Other		
CellASIC Onix Microfluidics Plates	Millipore	Cat#Y04D